For Reference

NOT TO BE TAKEN FROM THIS ROOM

For Reference

NOT TO BE TAKEN FROM THIS ROOM

Ex libris universitatis albertaensis

UNIVERSITY OF ALBERTA

QUAECUMQUE VERA

University of Alberta
Printing Department

Digitized by the Internet Archive
in 2018 with funding from
University of Alberta Libraries

https://archive.org/details/effectofmagnetic00ralp

Thesis
1964
#18

UNIVERSITY OF ALBERTA

THE EFFECT OF A MAGNETIC FIELD
ON
NORMAL SEGREGATION IN ALUMINUM(RICH)-COPPER ALLOYS

by

Ralph Clarence Dorward

A THESIS
SUBMITTED TO THE FACULTY OF GRADUATE STUDIES
IN PARTIAL FULFILMENT OF THE REQUIREMENTS
FOR THE DEGREE OF MASTER OF SCIENCE

DEPARTMENT OF MINING AND METALLURGY

EDMONTON, ALBERTA

APRIL 1964

ABSTRACT

The effect of a magnetic field on the solidification of aluminum (rich) - copper alloys was investigated using normal segregation as a criterion. The field strength was 34,000 oersteds applied perpendicular to the solidification direction for freezing rates ranging from 1/4 to 2 inches per hour. For a solidification velocity of 1 to 2 inches per hour there was an increase of 12 pct. in the segregation for the "field" solidified ingots compared to that for the normally solidified ingots. However, for freezing rates of 1/2 to 1/4 inches per hour the field did not affect the segregation to any observable extent. A theory has been presented which qualitatively explains the results.

ACKNOWLEDGEMENTS

The author wishes to express his gratitude to Dr. W. V. Youdelis for his guidance and supervision during the course of this project. He is also indebted to Mr. R.M. Scott who assisted with the photography, and to Professor E. O. Lilge for his helpful departmental supervision. Several members of the department offered helpful criticisms and discussions, especially Mr. D. R. Colton, M. Sc. and Mr. J. R. Cahoon, M. Sc. The assistance of Miss M. Sundin who typed the manuscript is also greatly appreciated.

The financial assistance provided by The Steel Company of Canada and The Consolidated Mining and Smelting Company is gratefully acknowledged.

TABLE OF CONTENTS

Page

I. INTRODUCTION 1

II. HISTORICAL REVIEW 3

A. Theoretical Considerations 3

(1) The Distribution Coefficient 3

(2) Normal Segregation 6

B. Experimental Observations 10

III. EXPERIMENTAL 12

A. Apparatus 12

(1) The Magnet 12

(2) Solidification Unit 12

B. Method 17

IV. RESULTS 19

V. DISCUSSION 32

VI. THEORY OF MAGNETIC EFFECTS 38

A. Thermodynamic Condiderations 38

B. Plasma Concept of a Metal 40

C. Irreversible Thermodynamics and the Diffusion Constraint 46

D. Consequences of Diffusion Inhibition 48

E. Energy Considerations 50

VII. SUMMARY AND CONCLUSIONS 53

BIBLIOGRAPHY 55

FIGURES AND ILLUSTRATIONS

Page

1. Partial Equilibrium Diagram with K<1. 4
2. Concentration Gradient in the Liquid Ahead of an Advancing Solid - Liquid Interface. 4
3. Segregation Patterns Corresponding to Various Solidification Conditions. 8
4. Photograph of the Pole - type Electromagnet. 13
5. Photograph of the Solidification Unit. 14
6. Photograph of the Drive Mechanism. 14
7. Cross section of the Solidification Unit. 15
8. Photograph of a Typical Unidirectionally Solidified Ingot. 20
9. Normal Segregation in the Al - 3.0 pct. Cu System for a Solidification Rate of 1 inch per hour and a Magnetic Field of 34,000 oersteds. 21
10. Normal Segregation in the Al - 3 pct. Cu System for a Solidification Rate of 4 inches per hour and a Magnetic Field of 34,000 oersteds. 22
11. Normal Segregation in the Al - 3.0 pct. Cu System for a Solidification Rate of 1 inch per hour and a Magnetic Field of 34,000 oersteds. 23

Page

12. Normal Segregation in the Al - 3.0 pct. Cu System for a Solidification Rate of 2 inches per hour and a Magnetic Field of 34,000 oersteds. 24

13. Normal Segregation in the Al - 2.9 pct. Cu System for a Solidification Rate of 1 inch per hour and a Magnetic Field of 34,000 oersteds. 25

14. Normal Segregation in the Al - 2.8 pct. Cu System for a Solidification Rate of 1/2 an inch per hour and a Magnetic Field of 34,000 oersteds. 26

15. Normal Segregation in the Al - 2.9 pct. Cu System for a Solidification Rate of 1/2 an inch per hour and a Magnetic Field of 34,000 oersteds. 27

16. Normal Segregation in the Al - 3.0 pct. Cu System for a Solidification Rate of 1/4 of an inch per hour and a Magnetic Field of 34,000 oersteds. 28

17. Normal Segregation in a two inch Ingot of Al - 3 pct. Cu for a Solidification Rate of 1 inch per hour and a Magnetic Field of 34,000 oersteds. 29

18. Macrograph of the Front End of an Ingot Showing Dendritic Growth and Entrapment. 30

19. Effective Distribution Coefficient vs. Solidification Rate. 31

Page

20. Partial Phase Diagram of the Al(rich) - Cu System Showing the Shift of the Liquidus Line. 34

21. Concentration Gradients and Temperature Distributions at the Solid - Liquid Interface. 49

I. INTRODUCTION

The electronic structure and transport properties of solids, such as galvanomagnetism, thermomagnetism, and the Hall effect have been successfully studied by the application of a magnetic field. This leads to the hypothesis that a magnetic field may affect solidification phenomena either through its effect on the equilibrium phase relationship of the alloy system, or through the irreversible transport processes of solidification. A study of solidification phenomena in a strong magnetic field should, therefore, elucidate crystallization mechanisms and the nature (electronic) of the solid - liquid system, provided the theoretical principles of alloy solidification and magnetic field interactions with electrically conducting fluids (magnetohydrodynamics) are correctly applied.

Previous work by D. R. Colton(1) on the solidification of binary alloys of bismuth with antimony and tin in a 13,000 oersted magnetic field, applied parallel to the direction of solidification, indicated that the field changed the amount of inverse segregation by about +100 pct. and −70 pct. respectively over the "no - field" results. J. R. Cahoon(2) investigated the effect of a magnetic field on inverse segregation in the aluminum (rich) - copper system, and found an increase in segregation of 60 pct. for a magnetic field strength of 34,000 oersteds. The magnitude of segregation was found to be independent of field direction. The observed segregation in the "field" solidified ingots for each system can be theoretically

calculated by the method of Kirkaldy and Youdelis (3) if the equilibrium phase diagram is altered by an appropriate shift in the liquidus curve, which is due to a proposed diffusion inhibition in the liquid caused by the field. In order to test further the validity of the alteration of the constitutional diagram it was decided to study the effect of a magnetic field on normal segregation in the aluminum (rich) - copper system, since this would allow better control (and evaluation) of the solidification variables. The amount of segregation, which is readily determined by ordinary chemical analysis, is related to the equilibrium phase relationship of the system. Any change in this relationship would be revealed by a change in the normal segregation pattern of a directionally solidified ingot.

II. HISTORICAL REVIEW

A. Theoretical Considerations

Normal freezing is a process of controlled solidification in which the entire body under consideration is melted and then frozen slowly and progressively from one end. Complications such as dendrite formation and inverse segregation present under conditions of rapid solidification (casting) are absent. In the following a brief resume of the theory of normal solidification is given.

(1) The Distribution Coefficient

Considering the partial equilibrium diagram shown in Figure 1, solidification of a binary liquid alloy of solute concentration C_o begins when the temperature reaches T_o. The concentration of the first solid to form is given by the intersection of the horizontal at temperature T_o with the solidus. It is convenient to introduce an equilibrium distribution coefficient, K_o, which is defined as the ratio of the equilibrium concentration of the solute in the solid (at the solid - liquid interface) to the equilibrium concentration of the solute in the liquid. The distribution coefficient may be greater or less than unity depending on whether the solute raises or lowers the melting point of the solvent. Figure 1 illustrates the case for K_o less than unity; whereas if the liquidus had a positive slope, K_o would be greater than unity. The distribution coefficient may be related in part to the distortion the solute atoms cause in the solid lattice. For K_o equal to unity

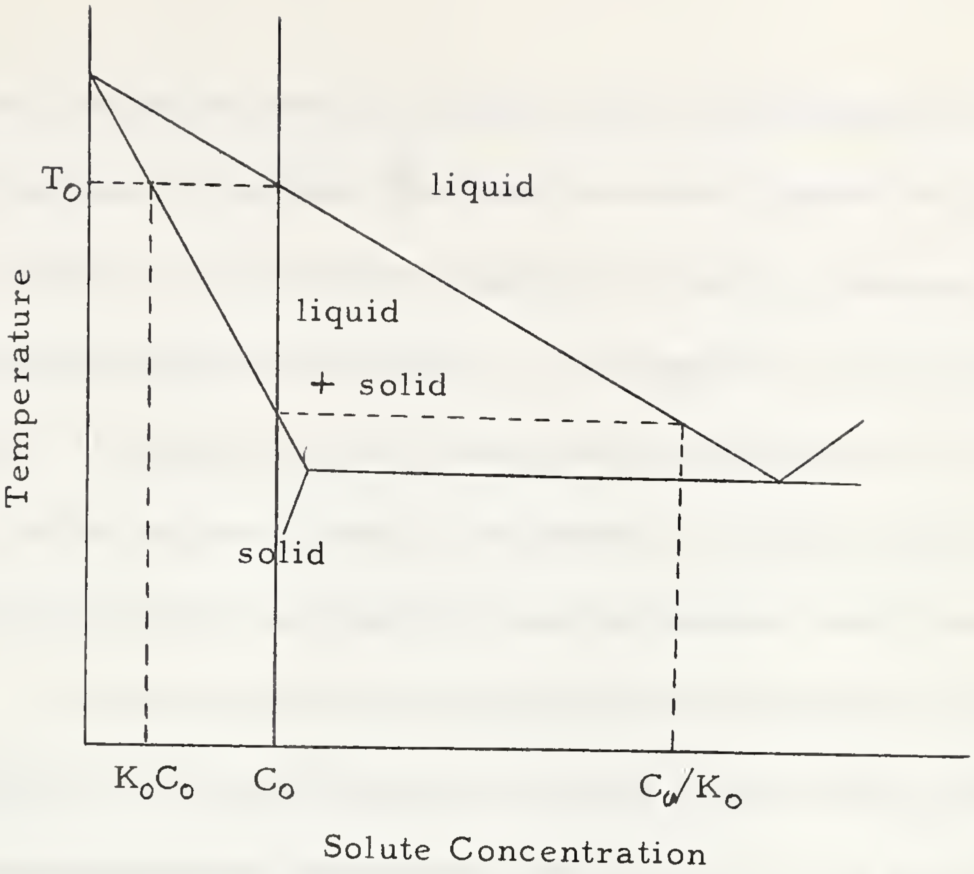

Figure 1. Partial Equilibrium Diagram with K<1

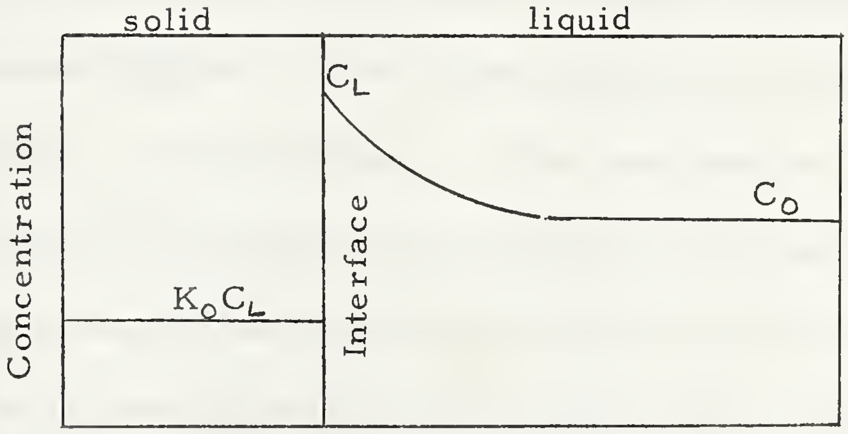

Figure 2. Concentration Gradient in the Liquid Ahead of an Advancing Solid - Liquid Interface

the solute creates no more distortion in the solid lattice than it does in the liquid, whereas if it is less than unity the solute lowers the melting temperature of the solid, thereby weakening the bonding between the atoms and increasing the interatomic distance. The opposite is true for K_o greater than unity. The departure of the distribution coefficient from unity is a measure of the degree of lattice distortion in a binary alloy system, assuming no electronic (valency or electro-chemical) effects are present.

Macroscopically the equilibrium distribution coefficient is rarely achieved in a real freezing process, for the reason that equilibrium conditions are not present (macroscopically) even for very slow solidification rates. Microscopically, however, local equilibrium is assumed to exist at the interface.(3) Consider the case for K_o less than unity. This corresponds to "rejection" of solute atoms by the solid as it forms, and therefore the solute concentration in the remaining liquid increases. This situation is illustrated in Figure 2, which shows the concentration profile near an advancing solid - liquid interface. At the interface the concentration freezing out in the solid is K_o times the concentration in the liquid. If diffusion is the only transport mechanism in the liquid there are two factors which influence the forms of the concentration gradient ahead of the interface:

(i) diffusion in the liquid tending to spread the solute throughout the melt at a rate determined by the diffusion coefficient D, and

(ii) the rate of freezing R, which acts as a source of solute at the interface.

When the solute concentration in the interfacial liquid reaches the value

C_o/K_o, steady state conditions exist because the concentration C_o of the liquid entering the "solidification zone" equals that leaving it in the solid. Tiller et al (4) derive the following expression for the concentration gradient for the steady state condition:

$$C_L = C_o \left[1 + \frac{1 - K_o}{K_o} e^{-\frac{R}{D}x'} \right] , \qquad (1)$$

where x' is the distance from the interface into the liquid.

Diffusion, however, is not the only transport mechanism in the liquid. There is usually some degree of convective mixing even in unstirred melts and a steady state condition is not attained. Any turbulence in the liquid affects the concentration gradient ahead of the solid - liquid interface by reducing its thickness. Thus, the solute concentration in the liquid at the interface will be lowered from that shown in Figure 2; and if solidification rates are sufficiently slow, the liquid will attain a uniform concentration through diffusion and convective mixing.

(2) Normal Segregation

As solidification proceeds along the charge, rejected solute accumulates in the liquid. Thus, due to this effect, and also because the liquid volume is being decreased, the liquid solute concentration rises. This, in turn, causes the concentration freezing out to increase since it is K_o times that in the liquid. If freezing is considered to proceed along a cylinder from one end to the other, an end - to - end segregation will

be produced in the solid ingot. This is known as normal segregation.

Depending on the conditions of freezing four different segregation forms can result as illustrated in Figure 3. They are:

(i) If solidification occurs slowly enough for equilibrium to be maintained there will be no segregation in the solid because time is allowed for complete diffusion. Diffusion rates in solid metals are so slow ($D \sim 10^{-9}$ cm.^{2}/sec.), however, that equilibrium freezing almost never occurs in practice.

(ii) When solidification proceeds slowly enough for diffusion in the liquid ($D \sim 10^{-5}$ cm.^{2}/sec.) to be complete but fast enough for diffusion in the solid to be negligible, Pfann$^{(5)}$ shows that the concentration gradient in the frozen solid is given by

$$C_S = K_o C_o (1-g)^{K_o - 1} \quad , \qquad (2)$$

where g is the fraction solidified. Under these conditions the maximum possible overall segregation is obtained.

(iii) When the freezing rate is rapid compared with diffusion and convective processes in the liquid, the distribution coefficient rises to unity and a plateau is produced in the segregation curve (cf. Equation 2). Under conditions of negligible convection, Tiller et al$^{(4)}$ show that the solute concentration in the solid for the initial transient is given by

$$C_s = C_o \left\{ (1-K_o)\left[1 - e^{-K_o \frac{R}{D} x}\right] + K_o \right\} \quad , \qquad (3)$$

where x is the distance measured from the starting point of solidification.

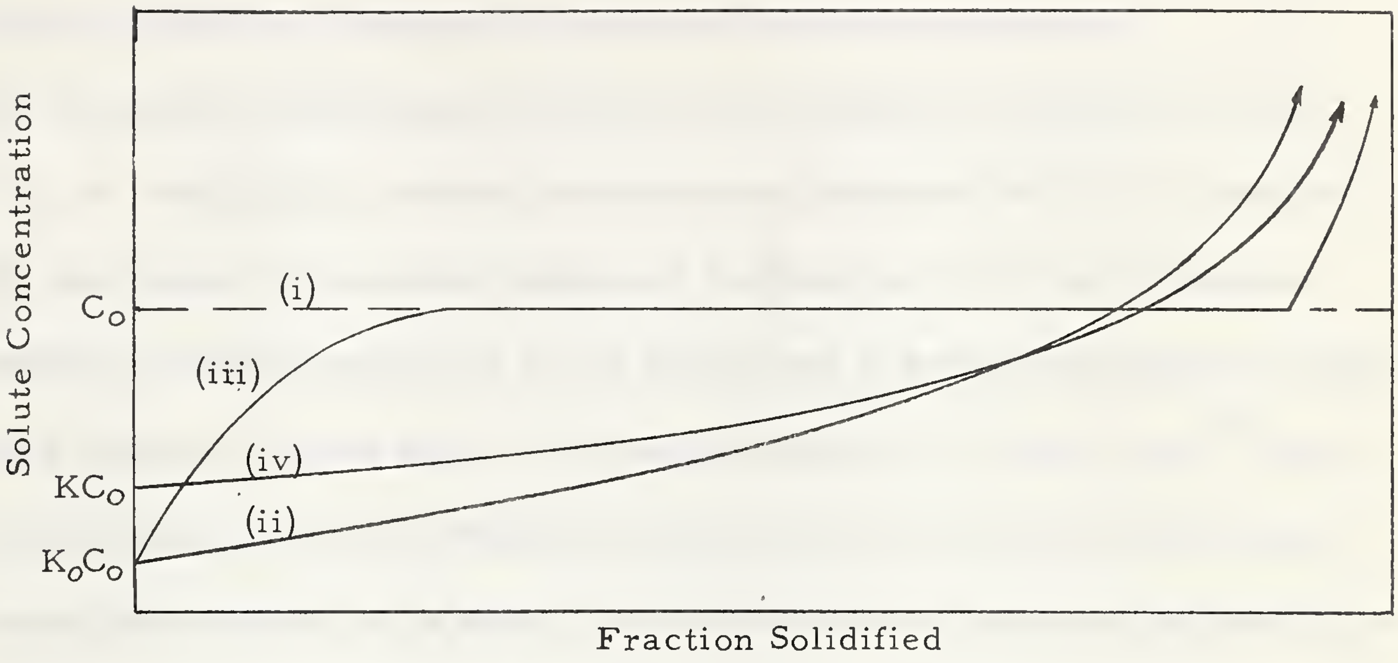

(i) Equilibrium Freezing

(ii) Complete diffusion in the liquid and negligible diffusion in the solid

(iii) Convective mixing in the liquid insignificant

(iv) Interfacial diffusion layer present with convective mixing in the liquid

Figure 3. Segregation Patterns Corresponding to Various Solidification Conditions.

This type of normal segregation is not often encountered in actual solidification because the freezing rates required are difficult to maintain without resulting in dendritic growth and inverse segregation.

(iv) In general solidification conditions are somewhere between (ii) and (iii), ie. the liquid is neither homogenous as assumed in Pfann's Equation (2), nor cored to the extend expressed in Equation (1). This is because convective mixing will occur in the liquid, and it will be homogenous except for a stagnant surface layer of average thickness δ. Burton et al$^{(6)}$ have shown that for this case Pfann's equation can still be used for the concentration distribution in the solid, but now an effective distribution coefficient, K, must be used in place of K_0 to take account of the effect of the stagnant unmixed layer. They derive the effective distribution coefficient as:

$$K = \frac{K_0}{K_0 + (1 - K_0)\, e^{-\frac{R}{D}\delta}} , \qquad (4)$$

Their derivation requires a planar interface, and complete mixing in the liquid alloy is assumed except for the interfacial layer of constant average thickness. The thickness of this layer depends on the efficiency of mixing in the bulk liquid, and transport of solute through it takes place only by diffusion. Dean et al$^{(7)}$ have shown that when the rate of solidification is relatively slow (in the order of 10^{-5} cm. per second), that the effective distribution coefficient approaches the equilibrium value.

B. Experimental Observations

During the past few years a great deal of experimental work has been conducted in the field of normal solidification. In the following a summary is given of some of the work substantiating the above theories.

The existence of a solute concentration gradient ahead of an advancing solid - liquid interface was shown by Burton et al.(8) They determined experimentally the effective distribution coefficients of various solute elements in germanium crystals grown from the melt. By varying the thickness of the layer through rotation of the crystal, they found that the effective distribution coefficient depended on growth conditions as expressed in Equation (4).

Using the expression for the steady state concentration gradient (Equation 1), Tiller et al(4) predicted the breakdown of a macroscopically smooth interface at a critical ratio of the temperature gradient in the liquid at the interface to the rate of growth. Walton et al(9) and Tiller and Rutter(10) experimentally verified this theoretical prediction by examining the solid - liquid interfaces of ingots which were solidified under controlled conditions. Convective mixing was assumed minimal because Wagner(11) had shown that this effect is not operable in the systems studied for the rates of solidification used (greater than 0.5 cm. per minute).

Yue and Clark(12) conducted directional freezing experiments on dilute magnesium alloys. They determined the effective distribution coefficients for the alloys at various freezing rates and discovered that the

normal segregation curves followed the theoretical expression given by Pfann (Equation 2), thus showing that for the case of partial mixing, K_o can be replaced by K. They also show that at very slow freezing rates the effective distribution coefficient approaches the equilibrium value. Similar experiments by Dean et al(7) have also led to the same general conclusions.

Weinberg(13) determined the solute distribution in the liquid during solidification of tin - silver alloys by quenching the residual liquid after freezing had commenced and then analyzing the solute concentration ahead of the "frozen - in" interface. He found that when convective mixing in the liquid had a negligible effect, the expressions of Tiller et al (Equations 1 and 3) were in good agreement with experiment. He also found that when convective mixing affects the solidification process, the segregation in the solid may be expressed by Pfann's equation, providing an effective distribution coefficient is used.

Recently Niessen et al(14) successfully applied Pfann's equation to normally solidified ingots of zinc - gold to determine the effective distribution coefficients corresponding to various growth velocities. They then extrapolated the experimental coefficients to zero rate of growth to obtain the equilibrium distribution coefficient of the system.

III. EXPERIMENTAL

A. Apparatus

(1) The Magnet

The magnetic field for the solidification experiments was obtained using a water - cooled, pole type electromagnet (see Figure 4) which was an adaptation of the Uppsala Electromagnet(15). The magnet supplied a maximum field of 35,000 oersteds uniform to ± 3 pct. over a cylindrical volume 3.5 inches in diameter and 1.5 inches in length. A thirty six kilowatt, direct current, constant voltage generator which gave a maximum voltage of 48 volts with a ripple of ± 2 pct. supplied power to the magnet.

(2) Solidification Unit

The alloys were solidified in the horizontal stainless steel tube and resistance furnace assembly shown in the photograph (Figure 5). A schematic drawing of the cross section of the unit is shown in Figure 7. The tube was 3 feet long and 3/4 of an inch in diameter, and was suitably connected to provide an atmosphere of argon. A copper cooling coil was positioned at the front end (where solidification was initiated) of the furnace in order to provide a reproducible temperature gradient at the solid - liquid interface. The alloy ingots were contained in a 4 inch long cylindrical, recrystallized alumina boat which was pushed out of the furnace by a moveable stainless steel rod 1/4 of an inch in diameter. The rod was

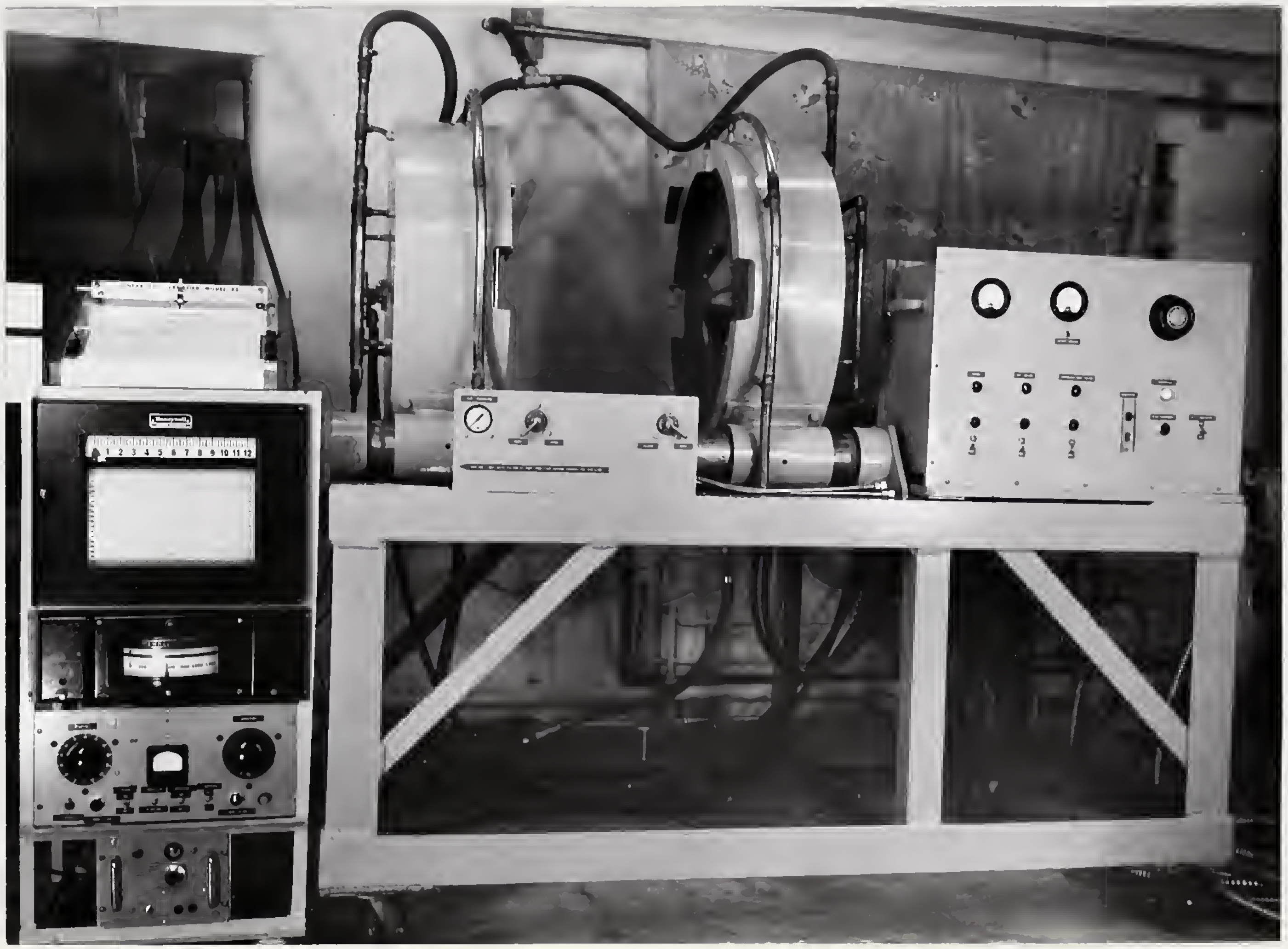

Figure 4. Photograph of the Pole - type Electromagnet.

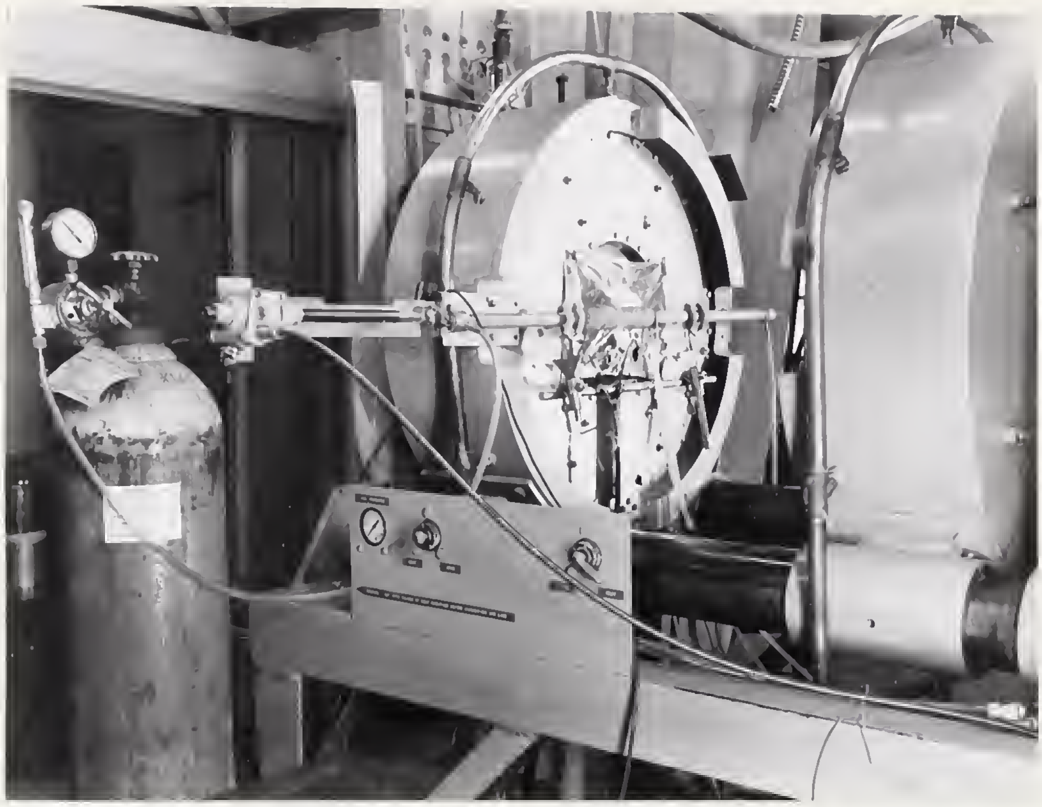

Figure 5. Photograph of the Solidification Unit.

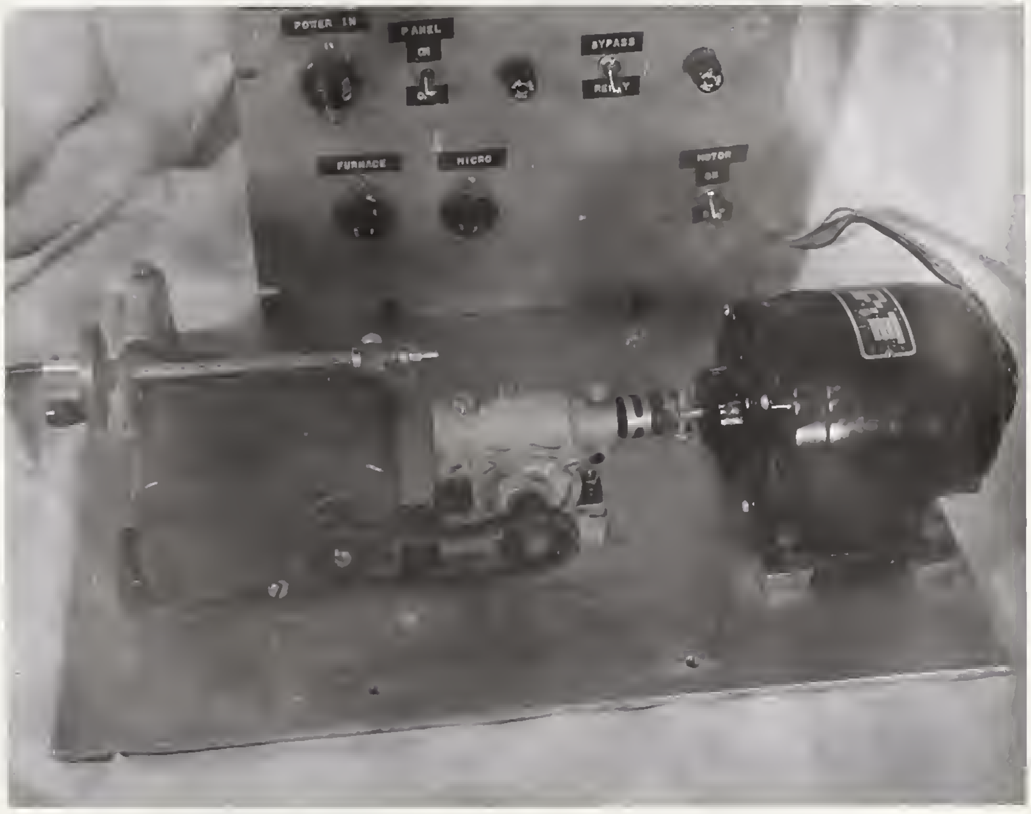

Figure 6. Photograph of the Drive Mechanism.

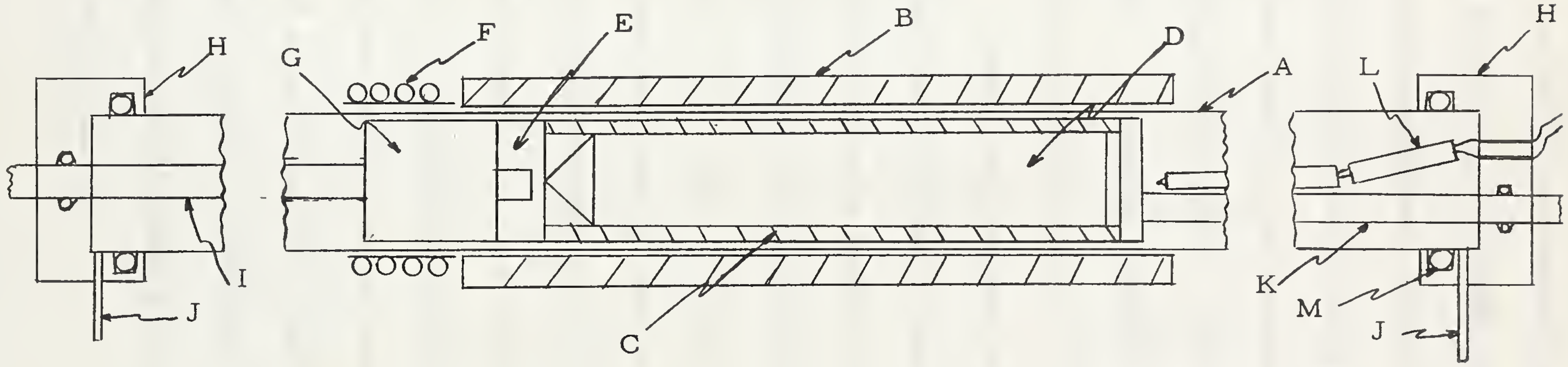

A	Stainless steel tube
B	Electrical resistance furnace
C	Recrystallized alumina boat
D	Al - Cu ingot
E	Tapered graphite end plug
F	Copper cooling coil
G	Copper heat sink
H	Tube end - seal
I	Stainless steel mixing rod
J	Argon atmosphere connections
K	Stainless steel drive rod
L	Chromel-P - Alumel thermocouple
M	"O" ring seal

Figure 7. Cross Section of the Solidification Unit

sealed at the end of the tube with an "O" ring. Another sealed stainless steel rod of the same dimensions was connected to the front end of the boat for mixing purposes. Steady travel rates were achieved with a synchronous electric motor and a Zero - Max (Figure 6) connected by a flexible drive shaft to a screw mechanism. The temperature was controlled by a stationary Chromel-P - Alumel thermocouple placed at the rear of the furnace. A Wheelco controller and a high - low variable transformer maintained the temperature to ± 2° C.

Initial experiments with a graphite boat indicated that the alloy supercooled when withdrawn from the furnace. This caused the solid - liquid interface to move rapidly along the first inch or less of the charge. Random nucleation occured in the initial portion of the melt resulting in entrapment of the solute during the ensuing rapid freezing. This effect has also been reported by Dean et al(7) and by Yue and Clark.(12) To largely eliminate random nucleation it was necessary to have good heat withdrawal through the front of the boat and low heat removal through the sides. Recrystallized alumina tubes with graphite end plugs were therefore used because of the relatively high thermal conductivity of graphite compared to alumina. The front end plug was also tapered in the manner described by Lawson and Nielsen(16) for growing single crystals. A copper block was fixed to the leading end for effective heat removal where solidification was initiated.

B. Method

The alloys were prepared in alundum coated silica crucibles by melting in an electric furnace. About four hundred grams of alloy containing 3 pct. copper[*] were prepared in each melt from aluminum (99.91 pct. purity) and electrolytic copper (99.99 pct. purity). The melts were thoroughly mixed by pouring them back and forth between two crucibles ten times. After mixing, the melts were degassed by bubbling with argon for approximately one minute. The alloys were then poured at a superheat of 50° C into a cool cylindrical graphite mould with dimensions 1 1/2 inches outside diameter and 5/8 inches inside diameter by 8 inches high. Four ingots were obtained from each melt. A cool mould was used so that solidification would proceed quickly from the sides along the length and not from the top or bottom in the manner of ingots quickly solidified unidirectionally. However, to eliminate any possible effects of inverse segregation, two inches were cropped from each end of the ingot where segregation, if present, would be greatest. The ingots were then machined down to fit into the alumina boat.

Before an experimental run the boat containing the alloy rod was positioned in the stainless steel tube so that the solid - liquid interface would be between the pole pieces of the magnet, and the system was purged with argon for twenty minutes. After the furnace was turned on and the

---

[*] All concentrations are in weight per cent.

alloy melted, the argon atmosphere was kept at a slight positive pressure for the duration of the run. Solidification did not commence until time was allowed for steady - state temperature gradients to become established. During this time the boat was rotated back and forth at five minute intervals by means of the stainless steel mixing rod. This process served to eliminate any gravity segregation formed on melting, and furthermore, it assured a uniform solute concentration lengthwise. The alloy was then solidified by pushing the boat through the furnace at the desired speed. Care was taken to reproduce exactly all conditions for the duplicate runs, one in a magnetic field of 34,000 oersteds perpendicular to the solidification direction and the other without a field.

The solidified ingots were sectioned and the swarfs of nine cuts along their lengths were collected for analysis. The sections were retained for metallographic examination. The iodide method of analysis (17) was used and all precautions for good volumetric procedure were followed to ensure good precision in the analysis. Corresponding slices of the duplicate ingots were analyzed at the same time to achieve the highest accuracy possible in the comparisons of the field and no - field results. The standard deviation of average samples was found to be 0.025 pct. copper which gives an accuracy in the difference between the field and no - field segregation curves of ±0.1 pct. copper.

IV. RESULTS

A photograph of a typical ingot is shown in Figure 8. The normal segregation curves for the 4 inch ingots are illustrated in Figures 9 to 16. Figure 17 shows the curves for the 2 inch ingots. The field and no - field curves are shown together for comparison. Figures 10 and 11 show the type of segregation that occurs if there is entrapment during the initial stages of freezing. Figure 11 is typical of the type of segregation obtained for a relatively fast solidification rate (in this case 4 inches per hour). A macrograph of the front end of an ingot solidified at this rate showed dendritic growth and entrapment as illustrated in Figure 18.

Since there was a slight amount of supercooling and entrapment at the beginning of solidification in each ingot, the segregation was extrapolated to the front of the ingot in order to obtain comparative effective distribution coefficients. The method of extrapolation balances the solute mass across the enriched (by entrapment) and depleted zones of the ingot. The values of the effective distribution coefficients corresponding to the different rates of solidification from 1/4 to 2 inches per hour are presented graphically in Figure 19. The K values are calculated using the relationship $C_S = KC_0$ for the entrapolated concentration at the ingot end. C_0 was determined by balancing the solute mass across the whole ingot.

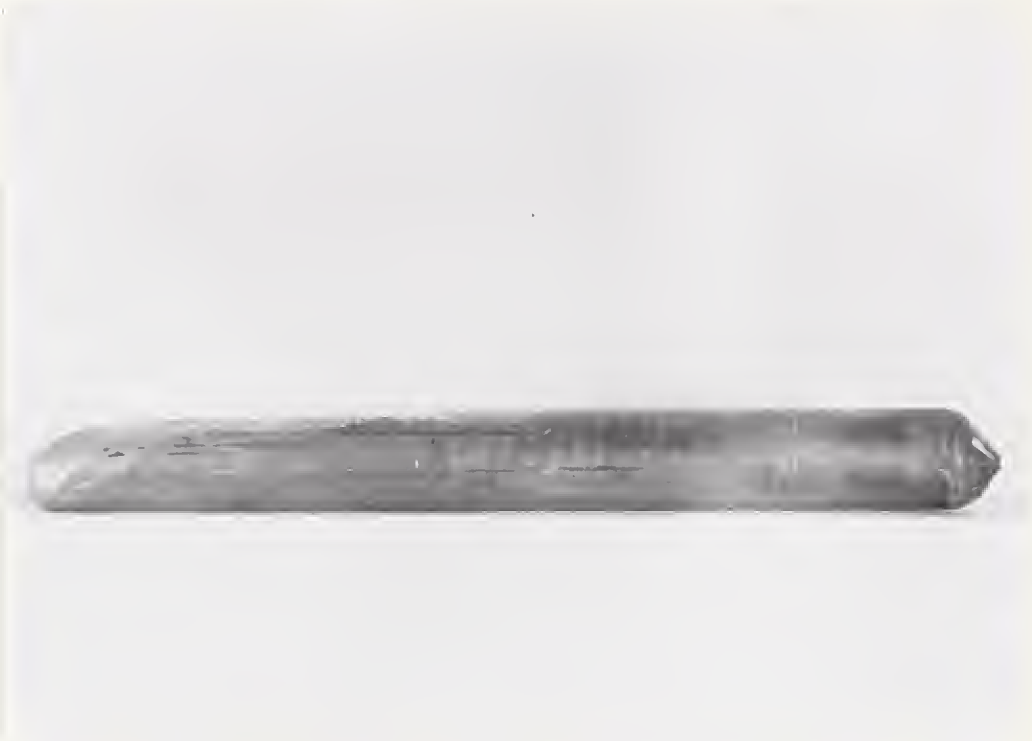

Figure 8. Photograph of a Typical Unidirectionally Solidified Ingot. (full size)

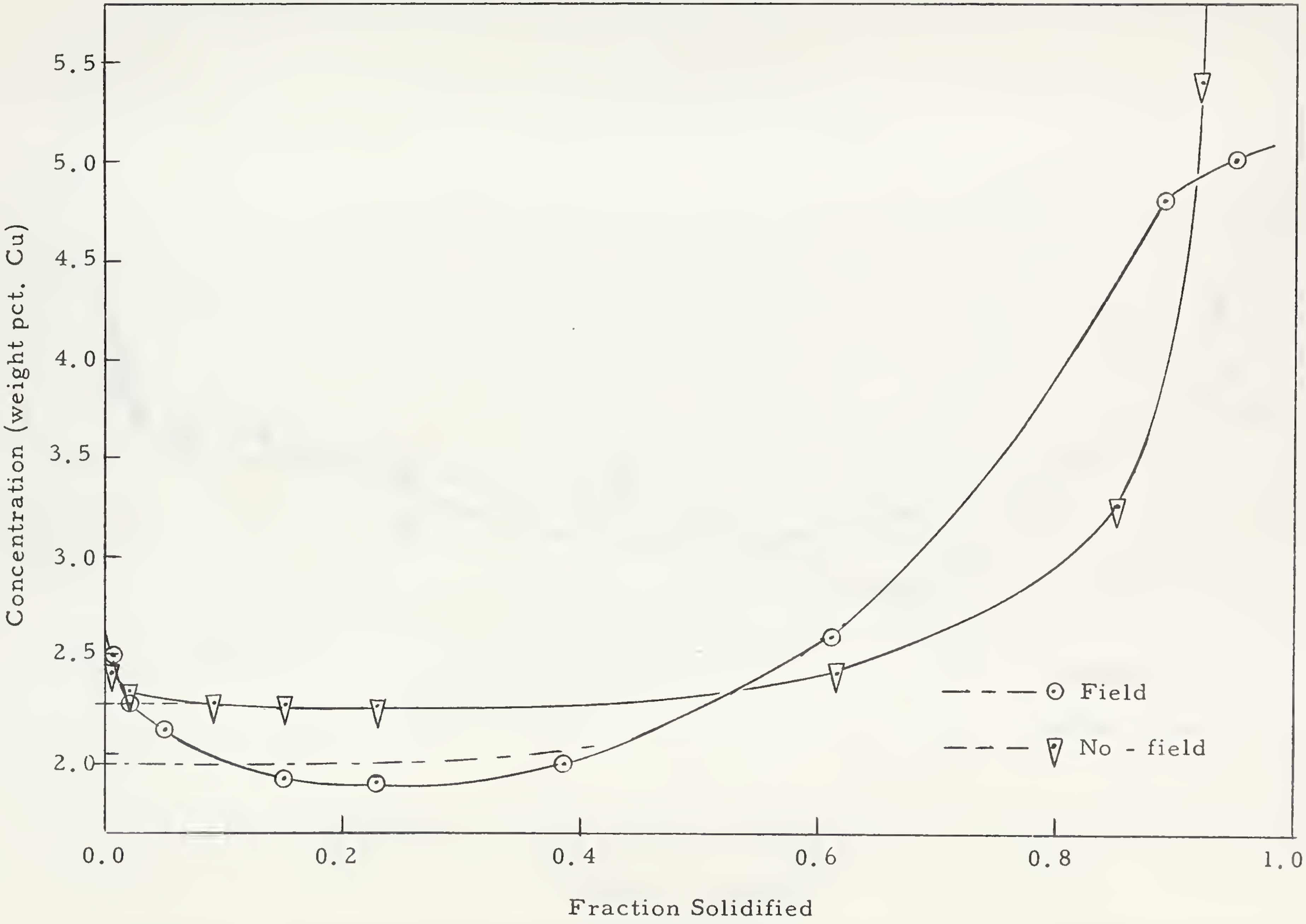

Figure 9. Normal Segregation in the Al - 3.0 pct. Cu System for a Solidification Rate of 1 inch per hour and a Magnetic Field of 34,000 oersteds.

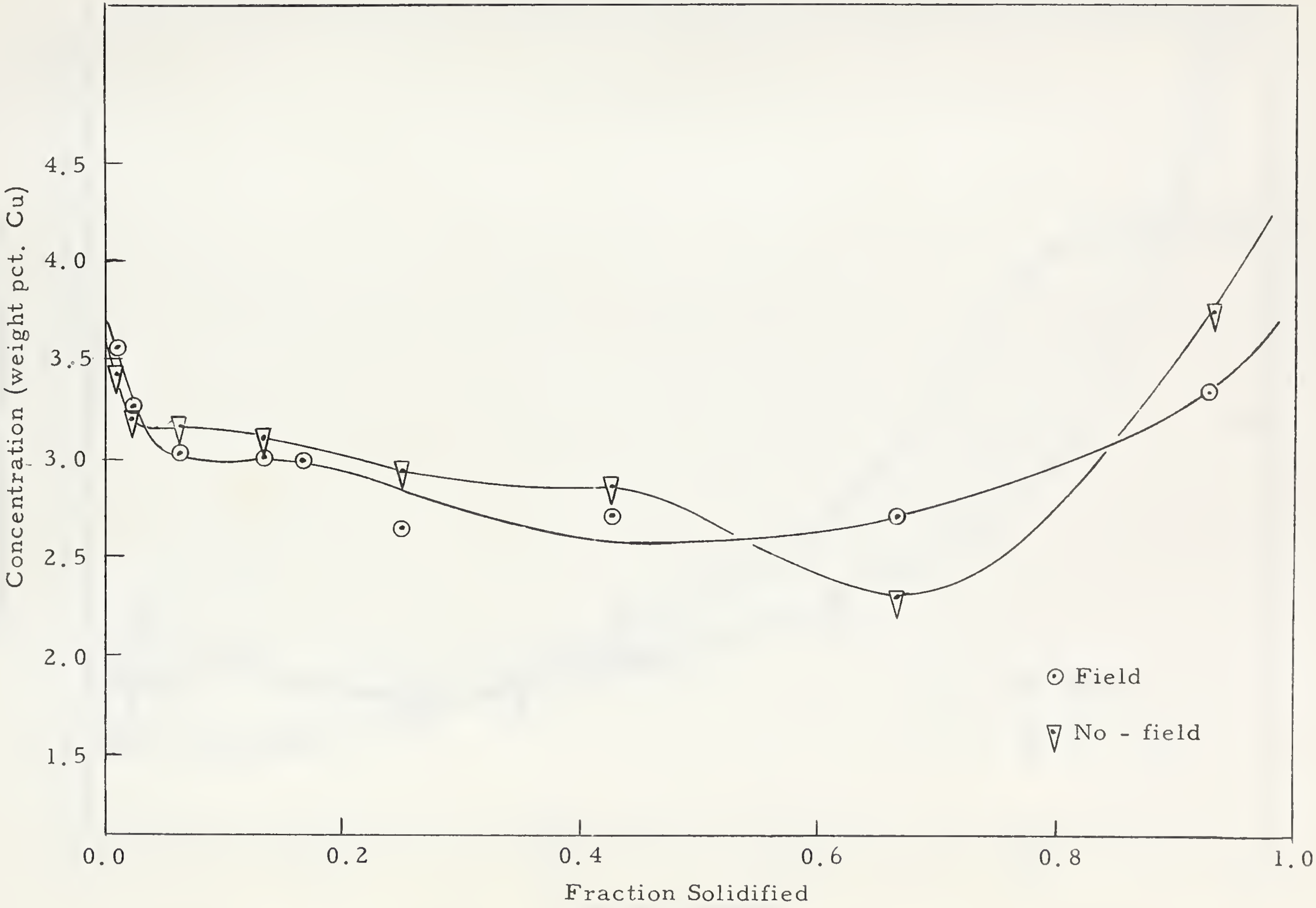

Figure 10. Normal Segregation in the Al - 3 pct. Cu System for a Solidification Rate of 4 inches per hour and a Magnetic Field of 34,000 oersteds

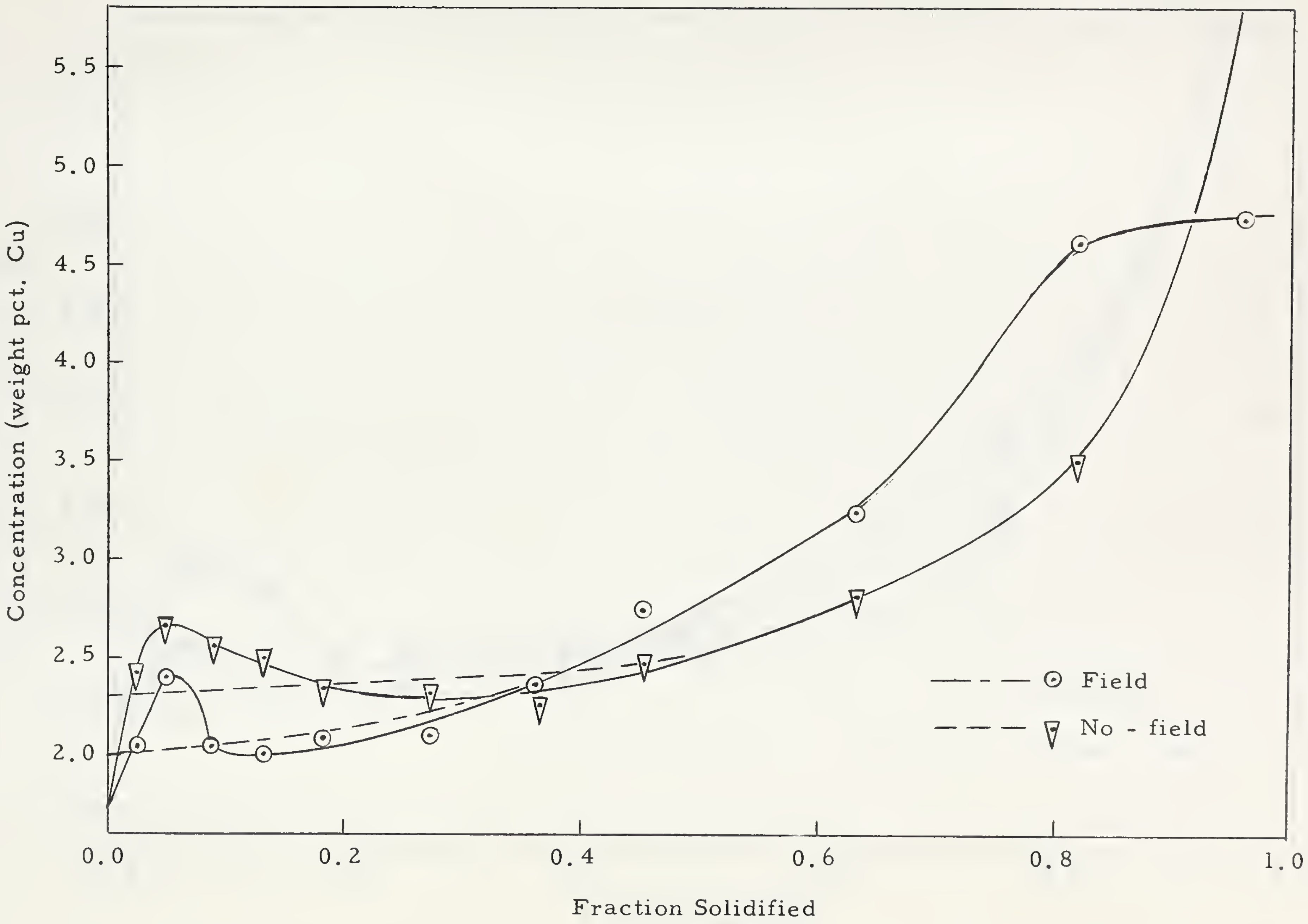

Figure 11. Normal Segregation in the Al - 3.0 pct. Cu System for a Solidification Rate of 1 inch per hour and a Magnetic Field of 34,000 oersteds.

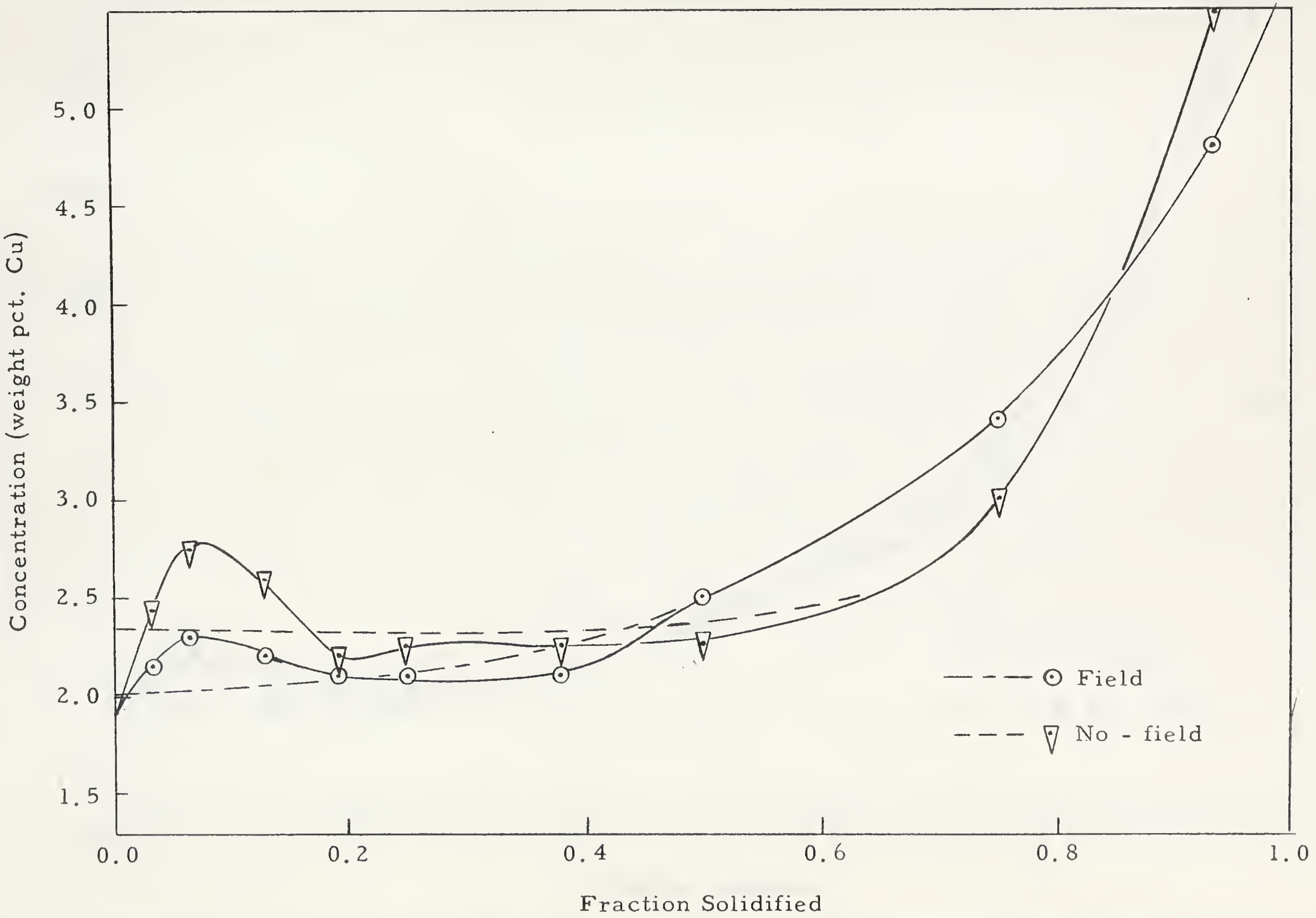

Figure 12. Normal Segregation in the Al - 3.0 pct.Cu System for a Solidification Rate of 2 inches per hour and a Magnetic Field of 34,000 oersteds.

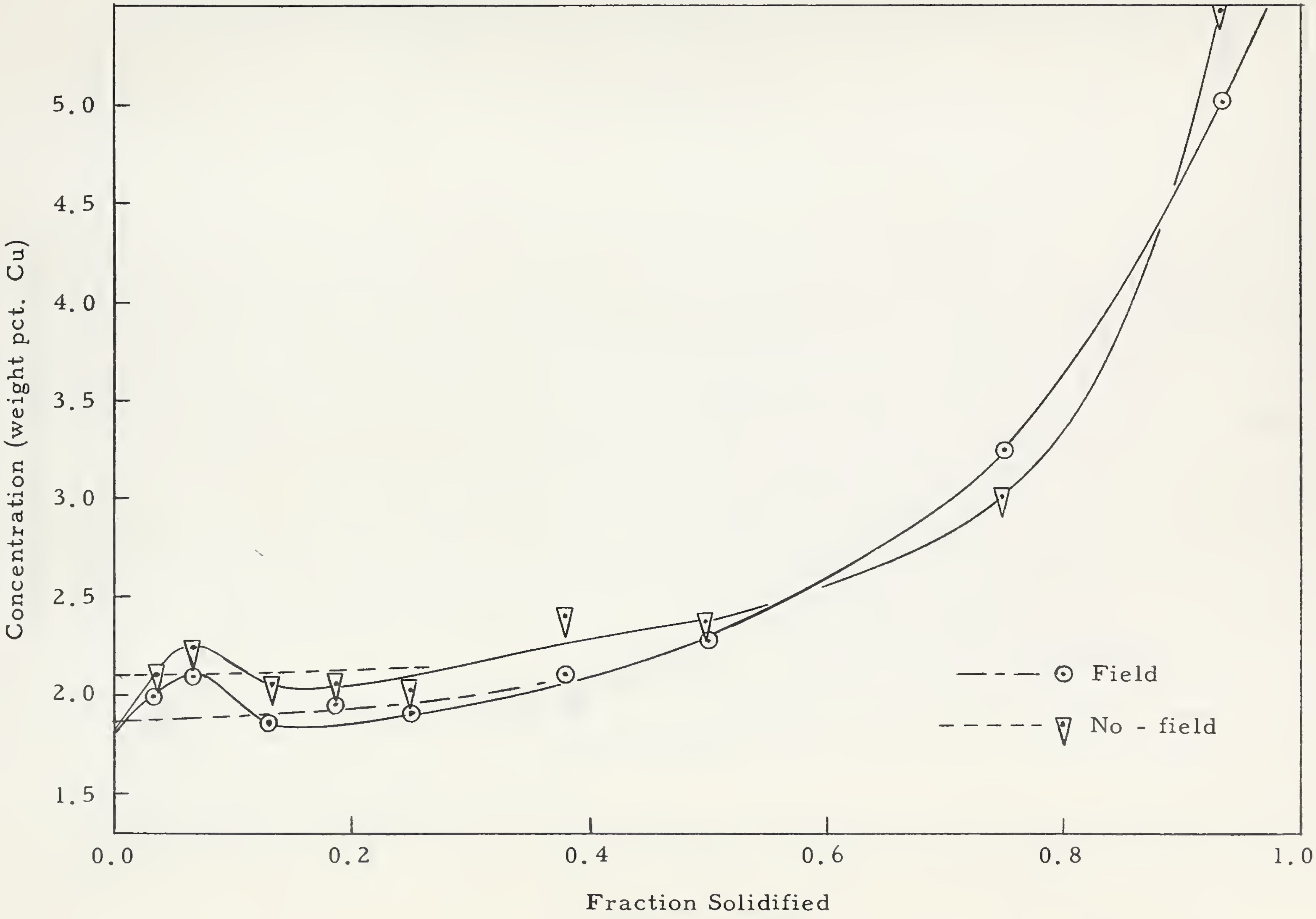

Figure 13. Normal Segregation in the Al - 2.9 pct. Cu System for a Solidification Rate of 1 inch per hour and a Magnetic Field of 34,000 oersteds.

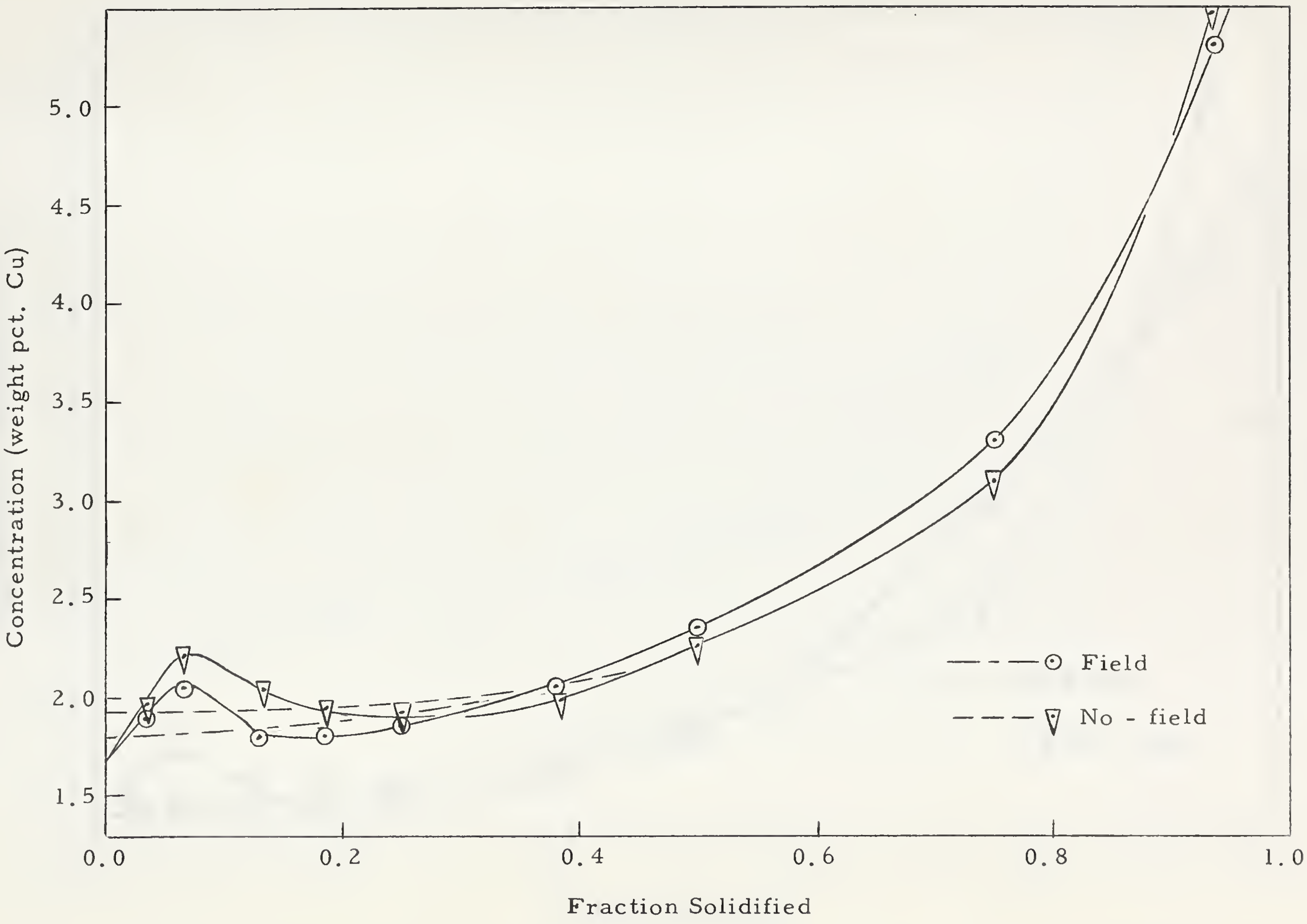

Figure 14. Normal Segregation in the Al - 2.8 pct. Cu System for a Solidification Rate of 1/2 an inch per hour and a Magnetic Field of 34,000 oersteds.

[illegible]

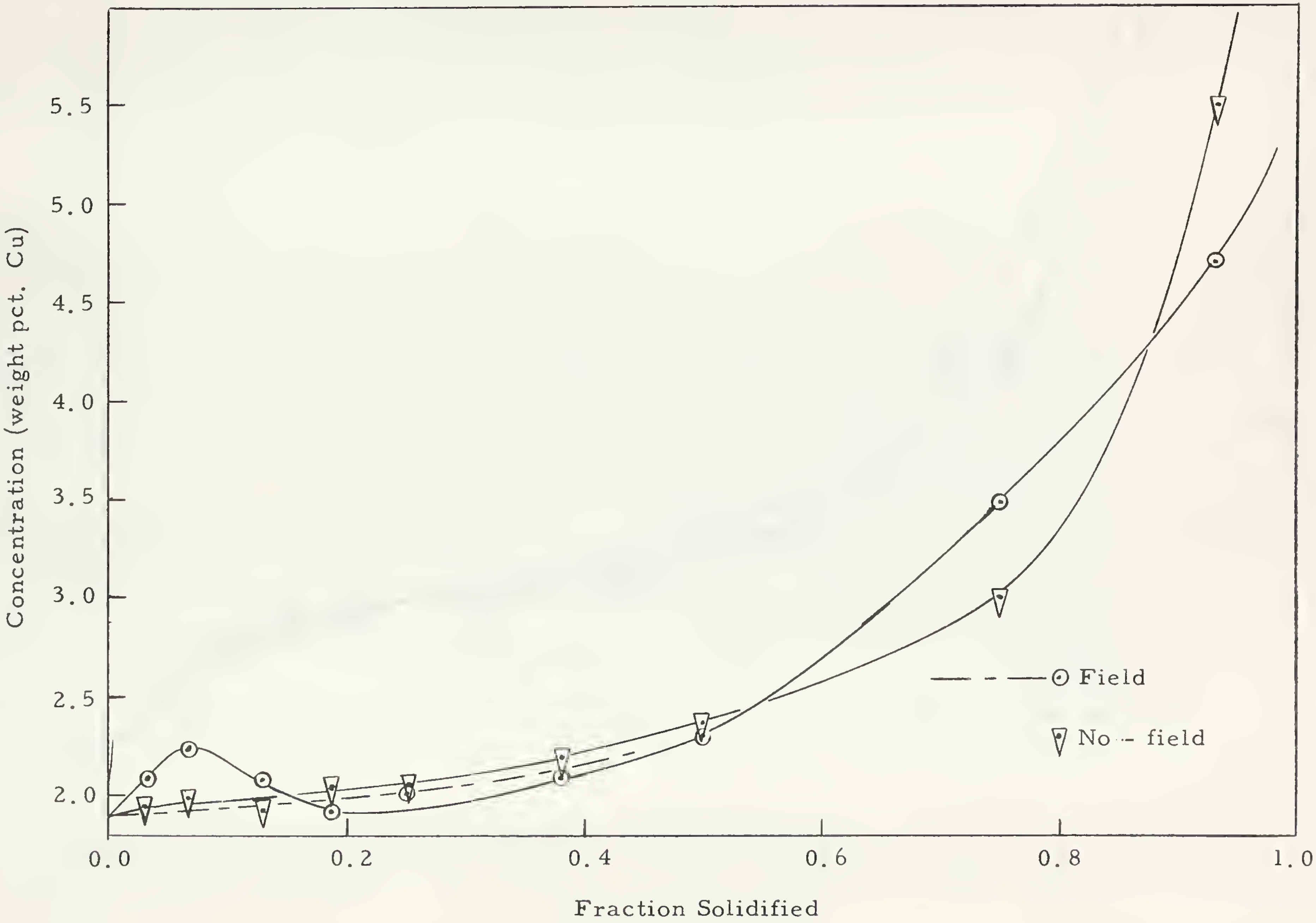

Figure 15. Normal Segregation in the Al - 2.9 pct. Cu System for a Solidification Rate of 1/2 an inch per hour and a Magnetic Field of 34,000 oersteds.

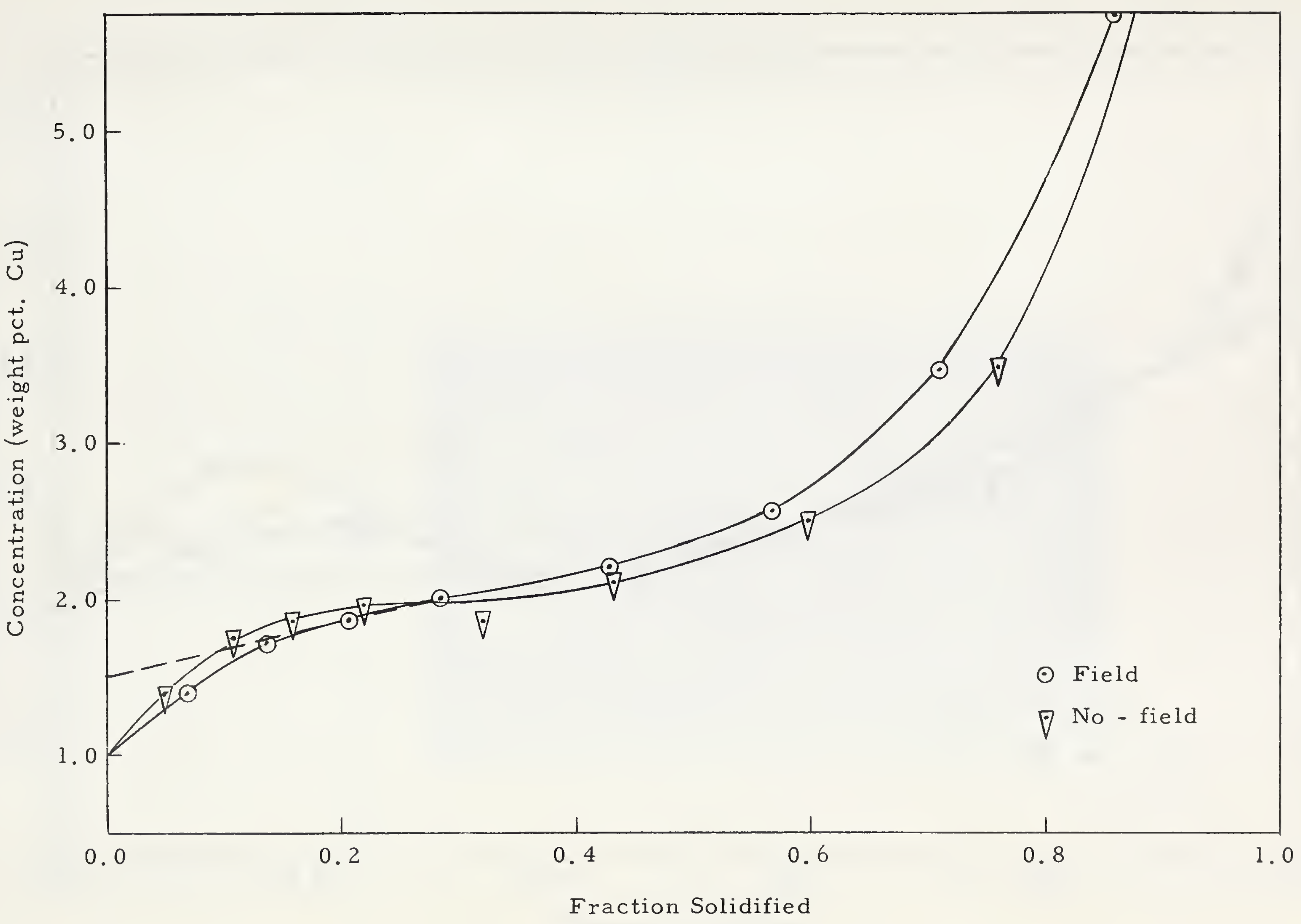

Figure 16. Normal Segregation in the Al - 3.0 pct. Cu System for a Solidification Rate of 1/4 of an inch per hour and a Magnetic Field of 34,000 oersteds.

[illegible]

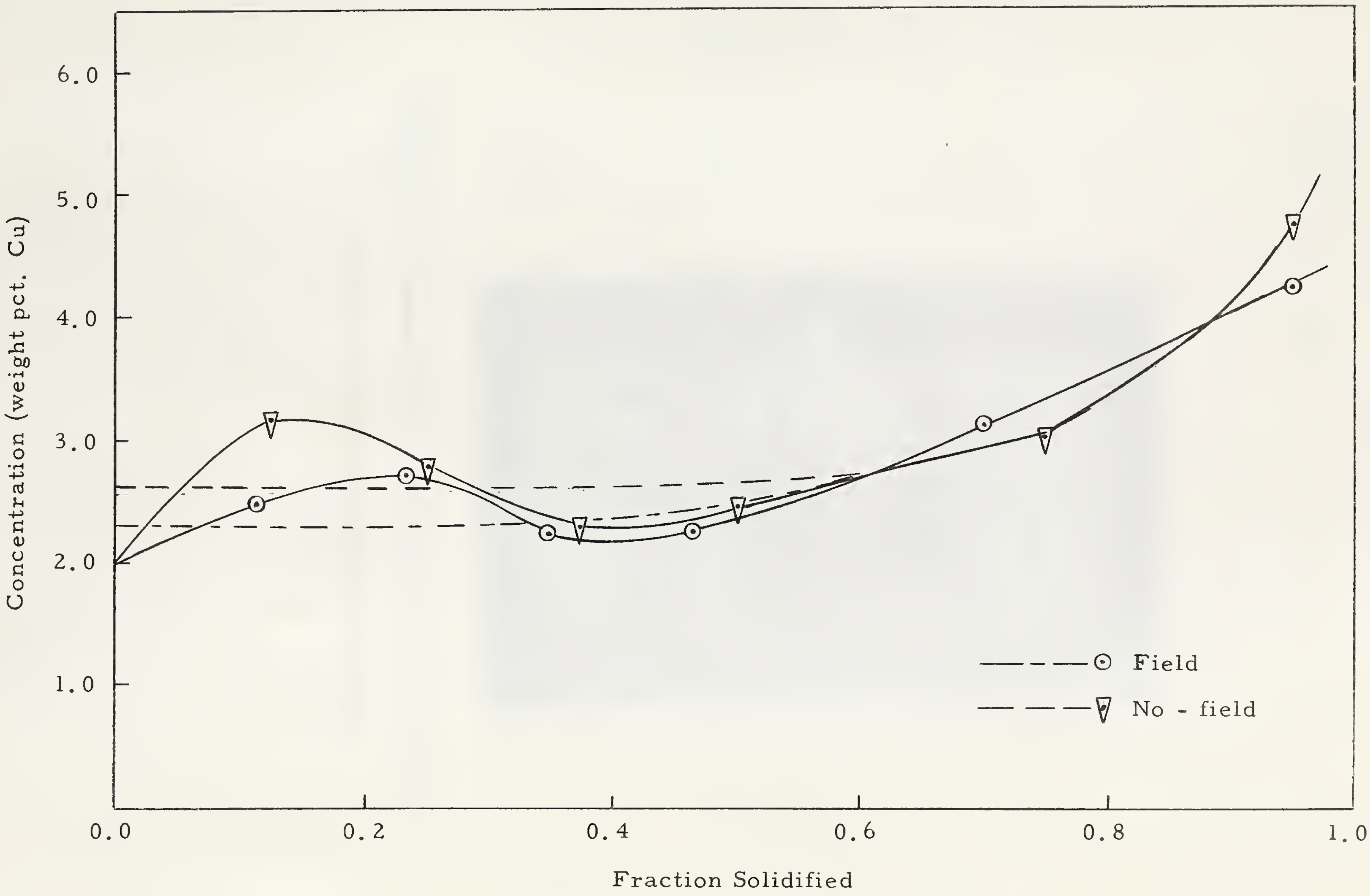

Figure 17. Normal Segregation in a two inch Ingot of Al - 3 pct. Cu for a Solidification Rate of 1 inch per hour and a Magnetic Field of 34,000 oersteds.

[illegible]

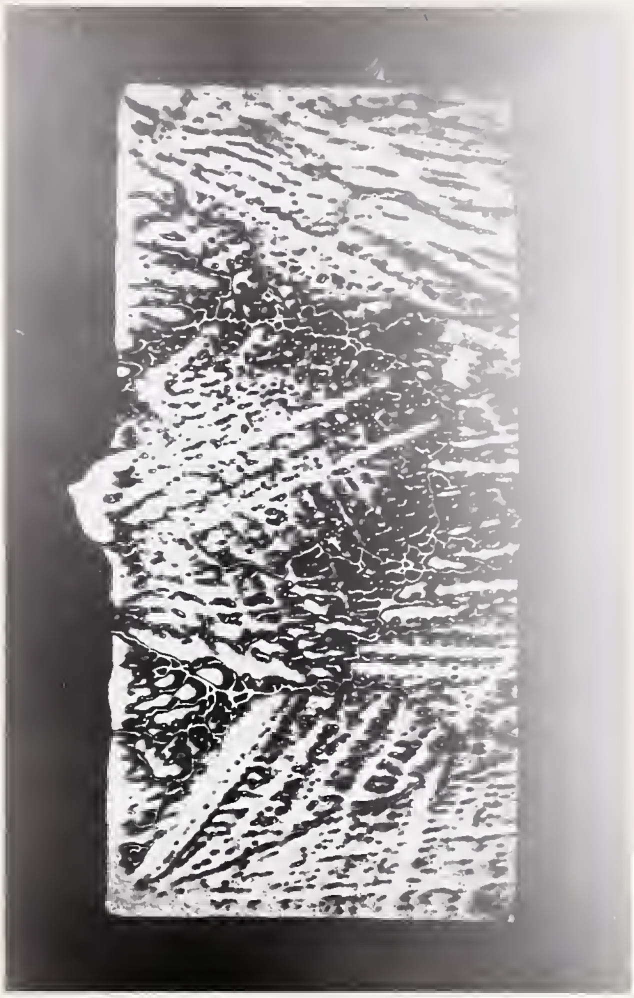

Figure 18. Macrograph of the Front of an Ingot Showing Dendritic Growth and Entrapment. (x7)

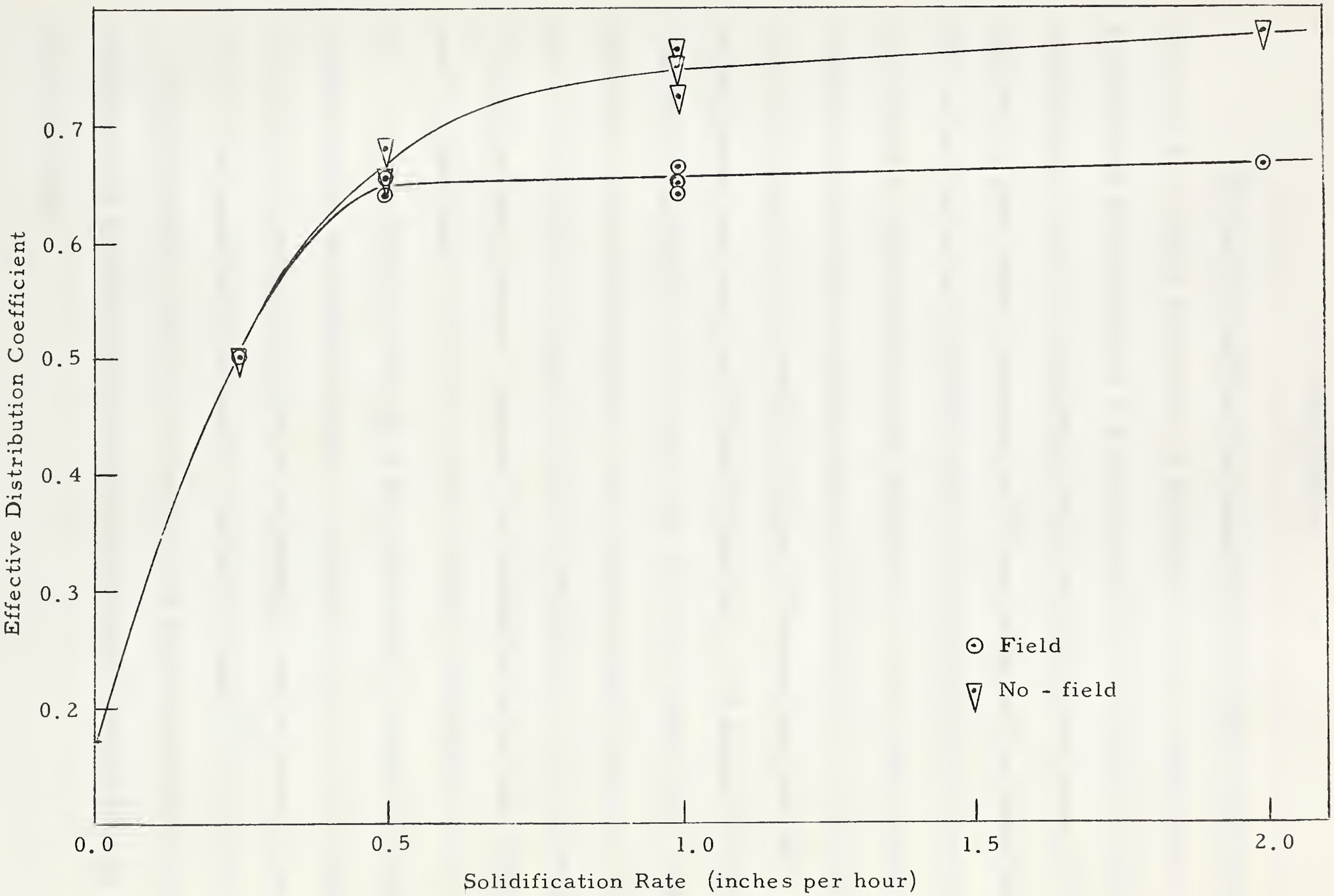

Figure 19. Effective Distribution Coefficient vs. Solidification Rate

V. DISCUSSION

Figure 19 shows that the magnetic field significantly increases the amount of normal segregation in aluminum - 3 pct. copper alloys at solidification rates exceeding 1/2 an inch per hour. The field solidified ingots have an effective distribution coefficient of 0.67 compared to 0.76 for the no - field ingots. Burton et al (6) have shown that extrapolation of this curve to zero rate of growth yields the equilibrium distribution coefficient since δ approaches zero (cf. Equation 4). For the alloy system studied here, the equilibrium distribution coefficient is 0.17. The curves of the field and no - field results in Figure 19 become coincident for solidification rates less than 1/2 an inch per hour, and appear to extrapolate to the equilibrium value of 0.17 for K_o at zero growth rate. The magnitude of the effect appears to level off at a freezing rate of 1 inch per hour. It is difficult to interpret results at solidification rates exceeding 2 inches per hour, however, because the mechanisms of normal growth tend to break down and dendritic growth becomes predominant (see Figure 10). It is interesting to note that in two cases where a substantial amount of supercooling was allowed to occur in the first liquid to solidify (Figures 9 and 10), that the amount of inverse segregation was increased by the field. This agrees with the results obtained by Cahoon (2) for inverse segregation studies of field - cast ingots. The field does not affect normal segregation to any observable extent for solidification rates less than 1/2 an inch per hour.

It remains to determine the process by which the magnetic field affects normal segregation for freezing rates greater than 1/2 an inch per hour. According to the relationship of Burton et al (Equation 4), the factors which determine the effective distribution coefficient for a given freezing rate R, are the liquid diffusion coefficient D, the equilibrium distribution coefficient K_o, and the diffusion layer thickness δ. Thus, it is possible to decrease K by adjusting one or all of these factors. A combination of changes is suspected since the effect is not the same for all freezing rates. The hypothesis put forth is that the equilibrium distribution coefficient is lowered via a decrease in the liquid diffusion rate of the solute atoms. The decrease in K also implies a change in the equilibrium phase relationship of the alloy system. It is further postulated that this change is a shift in the liquidus line of the phase diagram such as that shown in Figure 20 which results in a decrease in K_o. Cahoon(2) also found that it was possible to explain his inverse segregation results by such an alteration.

It is not possible, however, to determine quantitatively the extent of this liquidus shift from normal segregation results. At freezing rates of about 1 inch per hour a 12 pct. decrease in the effective distribution coefficient was observed with the field, ie. from 0.76 to 0.67, but it does not necessarily follow that an equal change occurs in the equilibrium distribution coefficient, K_o. This is because K is also dependent on the diffusion coefficient and if the latter is decreased as suggested, a larger

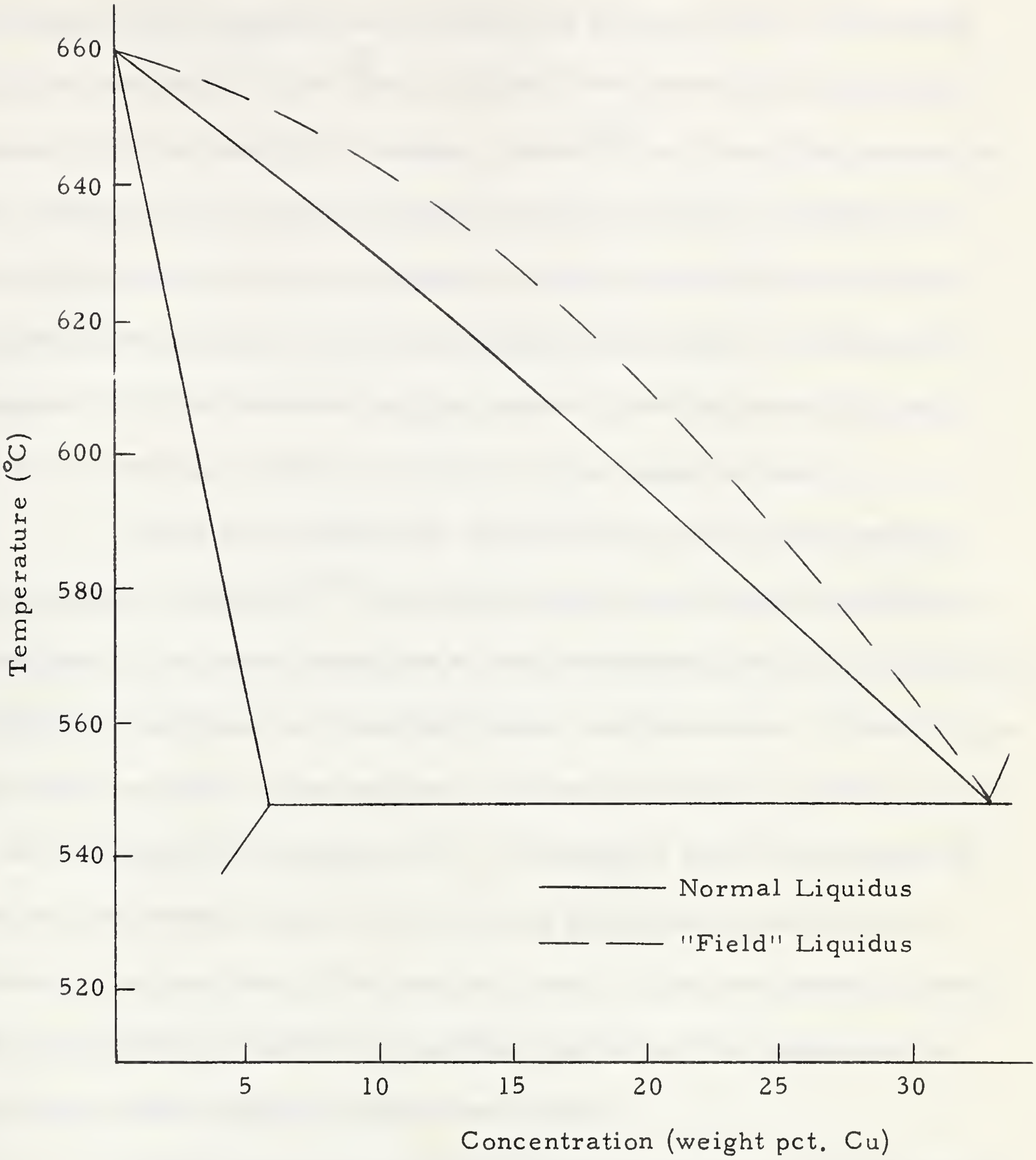

Figure 20. Partial Phase Diagram of the Al(rich) - Cu System Showing the Shift of the Liquidus Line.

decrease in K_o is required for the observed decrease in K. The change in K_o corresponding to the change in K will also depend on the effect of a magnetic field on convective mixing. Gupta(18) has shown that convective flow transverse to a magnetic field is severely inhibited. Inhibition of convective mixing tends to increase the effective distribution coefficient because the thickness, δ, of the interfacial solute layer is increased (cf. Equation 4). This indicates that the magnetic field decreases the equilibrium distribution coefficient even more than suggested above.

There is no observable "field" effect at very slow freezing rates because Dean et al(7) have shown experimentally that the diffusion coefficient of the solute atoms has an ever diminishing effect on the effective distribution coefficient as the solidification rate decreases. Therefore, at slow rates any effect of the magnetic field on the diffusion coefficient will not be manifested by a change in K. This explains why the field does not have any observable effect on the effective distribution coefficient for freezing rates less than 1/2 an inch per hour. In the next section a theory is presented which qualitatively justifies the shift of the liquidus of the equilibrium phase diagram of the alloy system.

It was considered necessary to establish whether the magnetic properties of the component atoms of the alloy studied had any effect on solidification under the experimental conditions. Since aluminum is paramagnetic and copper is diamagnetic, these metals will experience opposing forces when situated in a magnetic field gradient. Thus, normal segregation

may have been influenced by the sharp field gradient in the liquid metal outside the pole pieces of the magnet. For the 2 inch ingot run the liquid metal was entirely enclosed between the pole pieces and thus not under the influence of any significant magnetic field gradient. Figure 17 shows that the field still had the same effect on the segregation as it did with longer ingots solidified at the same rate. It may be concluded, therefore, that magnetic field gradients had no appreciable effect on normal segregation.

The segregation curves for comparative ingots extrapolate to the same concentration at the ingot end where solidification was initiated. This is in good agreement with the postulated theory because the field will not affect the solidification process until a diffusion layer has been established ahead of the solid - liquid interface. A finite amount of solid must be formed, however, before a solute concentration gradient can be built up. Therefore, the field should not be expected to have any influence on normal segregation in the initial portion of the ingot.

Another interesting feature of the results is the pattern of the segregation curves in the portion of the ingots which solidified last. In this region the field curves tend to level off and fall below the no - field curves. This may be attributed to the following factors:

(i) As shown by Tiller and Rutter,(10) there is a tendency for a planar interface to break down with an increasing solute concentration in the liquid. This results in dendritic growth, and the formalisms of normal solidification can no longer be employed to describe the freezing process.

(ii) The proposed diffusion inhibition in the magnetic field results in a higher solute concentration ahead of the solid - liquid interface.

The combination of these effects causes solidification in the field to proceed by columnar dendritic growth tending to give a macroscopically uniform solute concentration throughout the region.

VI. THEORY OF MAGNETIC EFFECTS

In the discussion of the results it was proposed that the magnetic field effect observed on normal segregation occurs via diffusion inhibition, with a consequent change in the position of the liquidus curve. We now consider the various possible effects of a magnetic field and show that the hypothesis of diffusion inhibition and equilibrium phase relationship change is a reasonable one.

A. Thermodynamic Considerations

The application of a magnetic field to a solidifying alloy may affect the constitutional diagram of the system through a change in the heat of solidification. The energy of a unit mass of material of specific magnetic susceptibility χ_m, placed in a magnetic field of strength H,* is given by(19)

$$E_m = \frac{1}{2} \chi_m H^2 \qquad (5)$$

The change in the heat of solidification of a metal solidified in a magnetic field will thus be

$$\Delta E_m = \frac{1}{2} \left(\chi_m^{l} - \chi_m^{s} \right) H^2 \quad , \qquad (6)$$

where the superscripts refer to the liquid and the solid respectively. The magnetic energy is small for weakly diamagnetic and paramagnetic substances, not exceeding a few calories per gram. Using aluminum as an example ($\chi_m^s = \frac{16.5}{10^6}$ and $\chi_m^l = \frac{12.0}{10^6}$),(20) the energy change upon solidification

---

* emu and cgs units are used unless otherwise specified.

in a 34,000 oersted field is 6 x 10^{-6} calories per gram. This is negligible compared to the heat of solidification of 94 calories per gram, and will have no observable effect on the constitutional diagram of the alloy system.

Another magnetic phenomenon which may affect the thermodynamics of an alloy system is magnetostriction. Magnetostriction is significant only in ferromagnetic materials and will not produce a significant bulk strain energy in paramagnetic or diamagnetic metals large enough that its effects will be noticeable in segregation work. For example $\Delta l/l$ for bismuth, a highly diamagnetic metal, is only of the order of 10^{-6} in a magnetic field of 10^4 oersteds.(21) This very small distortion of the lattice results in a correspondingly negligible energy change.

Finally it is necessary to consider the effect of a magnetic field on the solid solubility limits of an alloy system. Phase changes in alloys occurring at certain electron/atom ratios are attributed to a contraction of the Fermi sphere which lowers the electron energy.(22) This occurs when the Fermi sphere contacts the Brillouin zone boundary and part of the crystal structure changes to accomodate more solute atoms without increasing the electronic energy. If the magnetic field was to change the electronic energy of the alloy system, a particular phase change could occur, thus changing the solid solubility limits. A magnetic field coalesces into discrete degenerate levels the quasi - continuous energy levels of the conduction electrons in a metal, the degree of degeneracy depending on the field strength. As a result there is an increase in the

mean kinetic and exchange energies of the electrons. Dresselhaus$^{(23)}$ has shown however, that the electron energy increases appreciably only when the magnetic energy $\frac{h}{2\pi}\omega_{ce}$, equals the Fermi energy, where h is Plank's constant and ω_{ce} is the cyclotron frequency of the electron. The cyclotron frequency is given by

$$\omega_{ce} = \frac{eH}{m} , \tag{7}$$

where e is the charge of an electron and m is its effective mass. Since the Fermi level for metals is 1 to 10 electron volts, a field strength of about 10^8 oersteds would be required to effect any appreciable change in the Fermi energy. Thus, this mechanism will not account for the observed segregation results, and we must look elsewhere for an explanation of the magnetic effects on solidification.

B. Plasma Concept of a Metal

In its original and narrower sense the term plasma was applied to an ionized gas having a nearly equal number of positive and negative charges so that the state of the whole is electrically neutral. The term plasma is now generally taken to mean "the portion of a material body which is much larger than a Debye length and throughout which charged particles move".$^{(24)}$ The Debye length is a shielding distance beyond which the electric field of a charged particle is shielded by particles of opposite sign. A solid or liquid metal, therefore, may be considered to have plasma - like properties by virtue of the presence of the conduction

electrons. Since the translational freedom of the ion cores in the liquid is much greater than that of the ions in the solid, the liquid is nearer to the original concept of a plasma than is the solid.

The study of the interaction of magnetic fields with plasmas or moving conducting fluids, if the continuum property is present, is known as magnetohydrodynamics. It is necessary to examine the magnetohydrodynamic forces in a conducting fluid and their possible effects on the transport processes of solidification. In a liquid metal under the influence of a magnetic field the ensemble of electrons and ions can be viewed as charges which move across the magnetic lines of force, and they thus experience electromagnetic forces that accelerate them in a direction perpendicular to both the field lines and their instantaneous direction of velocity. The magnetohydrodynamic equations of motion for a plasma must contain quantities such as pressure, density, viscosity, and constraints imposed by the magnetic field variables. Thus, Maxwell's equations must be coupled with the hydrodynamic equations to define the motion to the bulk plasma.

The magnetohydrodynamic equation of motion is given by(25)

$$\rho \dot{\vec{v}} + \rho(\vec{v} \cdot \vec{\nabla})\vec{v} = -\vec{\nabla} p + \rho \vec{g} + \rho \nu \nabla^2 \vec{v} + \mu \vec{j} \times \vec{H} , \qquad (8)$$

where:

$\vec{v}$ = macroscopic velocity of the fluid

ρ = density of the fluid

p = pressure

ν = kinematic viscosity of the fluid

μ = permeability of the plasma

$\vec{g}$ = gravitational acceleration

$\vec{H}$ = magnetic field strength

$\vec{j}$ = macroscopic current density

Along with Equation (8) which is derived from the Boltzmann transport equation,$^{(26)}$ Maxwell's equations relating the electrical and magnetic fields, $\vec{E}$ and $\vec{H}$, are required for the complete description of the system. However, for the case of finite resistivity and constant magnetic fields, the system may be described by Equation (8) and the equation for the macroscopic current

$$\vec{j} = \sigma(\vec{E} + \mu\vec{v} \times \vec{H}) , \tag{9}$$

where σ is the electrical conductivity of the fluid. The electromagnetic force $\mu\vec{j} \times \vec{H}$ in Equation (8) is often referred to as the ponderomotive force. It tends to impede motion across the lines of force. If $\vec{j}$ is replaced by Equation (9) this force becomes

$$\mu\vec{j} \times \vec{H} = \mu\sigma(\vec{E}_\perp \times \vec{H} - \mu H^2\vec{v}_\perp) , \tag{10}$$

where $\vec{E}_\perp$ and $\vec{v}_\perp$ are the components of $\vec{E}$ and $\vec{v}$ transverse to the magnetic field. The quantity $\mu\sigma H^2\vec{v}_\perp$ is the induction drag tending to destroy motion across the lines of force, and is regarded as a magnetic viscosity. This induction drag will inhibit diffusion in the liquid only to the extent that

there is bulk motion of the fluid associated with diffusion. Diffusion in liquid metal systems is relatively slow and density changes are small however, so the effect of the magnetic viscous force on solidification will be negligible.

Although the macroscopic forces may be negligible, the magnetic forces on the individual particles remain and will affect their relative motion. A charged particle describes between collisions a spiral path around a magnetic line of force. Equation (8) is only valid when the gyration radius of a particle is much larger than its mean free path. If the field strength is such that the gyration radius is of the order of a mean free path, the system must then be described by the fundamental kinetic equations of plasma dynamics.

A pressure gradient, $\vec{\nabla} p$, in a plasma under the influence of a magnetic field is responsible for various drift motions of the plasma perpendicular to the field. Neglecting particle collisions, the velocity of this drift perpendicular to $\vec{H}$ and $\vec{\nabla} p$ is given by (27)

$$\vec{v}_\perp = \frac{\vec{H}}{\mu H^2} \times \left(-\vec{E} + \frac{\vec{\nabla} p_i}{e n_e} \right) , \tag{11}$$

where $\vec{\nabla} p_i$ is the pressure gradient of the ion cores and n_e is the electron density. If collisions between electrons and ions are considered, there will be an additional contribution to $\vec{v}_\perp$ given by (28)

$$\vec{v}_\perp' = \frac{-\vec{\nabla} p}{\sigma_\perp \mu^2 H^2} , \tag{12}$$

where $\vec{\nabla} p$ is the total pressure gradient and $\sigma_\perp$ is the electrical conductivity transverse to the magnetic field. Thus, for liquids of finite conductivity there are normally two drift components, one parallel to the pressure gradient and one perpendicular to it. The component of $\vec{v}_\perp$ parallel to $\vec{\nabla} p$ represents a net outward drift of the plasma. Collisions between like particles do not to a first approximation contribute to any alteration of the density distribution since an encounter between two identical particles shifts the two guiding centers (orbital centers of the gyrating particles) by equal and opposite amounts.(29)

"Diffusion" caused by these drift motions is flow resulting from the motion of ions and electrons together, not movement of one species relative to another. It is therefore not possible to make a comparison of the flow component along $\vec{\nabla} p$ in Equation (12) with normal diffusion velocities in liquid metals. Equation (12) does, however, show the nature of diffusion inhibition. The extent of flow or "diffusion" parallel to the density gradient is inversely proportional to H^2, causing flow along the gradient to vanish for very high field strengths.

A more useful insight into the diffusion mechanism can be obtained if the alloy is viewed basically as a two fluid plasma of ions and electrons. The relative effect of the field on the cyclic motion of the electrons to its effect on the ions is proportional to the inverse ratio of their masses. The motion of the electrons only need be considered, for through the requirement of electrical neutrality, the electrons will determine

the motion of the ions (ambipolar diffusion). A concentration gradient at the solid - liquid interface results in a free electron gradient (providing the valencies of the component metals are different), which in a magnetic field is assumed to behave as a plasma density gradient. If the electrons are able to describe at least a turn or so of their spiral paths between successive collisions, their average displacements along the density gradient will be greatly reduced by the presence of the field.(30) If this situation is realized in a liquid metal in a moderate magnetic field, the immoblization of electron motion across the field would in turn determine the ion motion because of the basic requirement of electrical neutrality. Assuming that the zone structure is largely retained in the liquid state,(31) the calculated value of the gyration radius for an electron moving at the Fermi velocity in a field of 10^4 oersteds does approach the normal mean free path of the electron. The extent to which the charge distribution within a plasma can deviate from the equilibrium distance is the Debye distance, h_D, given by

$$h_D = \left(\frac{KT}{4\pi n_e e^2} \right)^{1/2} , \qquad (13)$$

where n_e is the electron density, k is Boltzmann's constant and T is the absolute temperature. In metals this distance is only the order of an angstrom unit if the thermal energy, kT, is replaced by the Fermi energy. Therefore, the heavy positive ions will be confined by the restrained electrons, and diffusion will be inhibited.

---

[*] A useful approximation for evaluating h_D by which order of magnitude agreement is obtained with more refined theories (Thomas-Fermi approximation of the charge potential for example)

C. Irreversible Thermodynamics and the Diffusion Constraint

In order to determine the effect of diffusion inhibition on the solidification process, the irreversible thermodynamics of the process must be considered. The thermodynamic principle governing an irreversible process is that the rate of entropy production is positive definite and a minimum.(32) The minimum rate of entropy production may be described by a variational principle, where variation is made with respect to the free thermodynamic forces.(33) The rate of entropy production per unit volume is represented as a bilinear function of the fluxes $\vec{J}_i$ and their conjugate forces $\vec{X}_i$. For solidification of a binary alloy these fluxes and forces are those related to the temperature gradient, the free energy difference for the liquid - solid reaction, and the chemical potential gradient. Kirkaldy(34) has shown that the variational principle generates Le Chatelier's principle of moderation in the presence of constraints for steady state, heterogenous convective systems such as crystal growth in binary alloys. The variational principle can also be used to define the process path of non - stationary heterogenous dissipative systems.(35) The entropy production rate is still a minimum, but it must now be consistent with the external dynamic constraints that assure a non - zero transformation rate.

The system under consideration has an undefined internal constraint associated with the inhibited diffusion process which is coupled in some unknown way to the interfacial reaction. This internal constraint

may be replaced by a suitable external mathematical one which allows conventional phenomenological formalism and so permits definition of the system in terms of variational principles.(35) The actual process path the system will chose will be that which is compatible with the dynamic constraints and which tends to minimize the rate of entropy production.

de Groot gives for the entropy production rate, σ, of a non-polarized continuous system undergoing a thermal conduction - diffusion - viscous flow process in a electromagnetic field the following expression:(36)

$$\sigma = \left(-\vec{J}_q \cdot \mathrm{grad}\, T - \sum_{k=1}^{n} \vec{J}_k \cdot T\, \mathrm{grad}\, \frac{\mu_k}{T} + \vec{i} \cdot \vec{E}' - \Pi : \mathrm{grad}\, \vec{v}\right) \Big/ T \geq 0 \qquad (14)$$

Equation (14) consists of a sum of products of fluxes and thermodynamic forces containing terms arising from heat conduction, diffusion, electric conduction, and viscous flow respectively. $\vec{E}' (= \vec{E} + \vec{v} \times \vec{H})$ is the electric field relative to the axis moving at the velocity $\vec{v}$ of the mass, Π is the viscous pressure tensor, and u_k represents the chemical potentials of the diffusing substances. The entropy production rate differs from that without an electromagnetic field only by the inclusion of the electric conduction term, $\vec{i} \cdot \vec{E}$. This is a Joule heat dissipation term arising from Hall currents. The effect of the field is found in the diffusion and the viscous flow term since it is assumed that $\vec{J}_k$ and the transverse component of $\vec{v}$ are reduced. The rate of entropy production increase $\vec{i} \cdot \vec{E}/T$ should be equal to the decrease in the diffusion entropy factor. If the solidification time for the system is unaltered by the field, the diffusion and viscous flow terms will decrease the total entropy production in the system because the Joule heat will be dissipated. Heat conduction should play the dominant

role in energy dissipation for solidification in a magnetic field because diffusive flow is inhibited whereas transverse heat flow is affected considerably less than mass transfer itself. Non - convective heat flow at liquid metal temperatures involves momentum transfer largely via vibrating ions,(37) so its component transverse to the field will not be affected to the same extent as would mass transfer. The decreased diffusion and viscous flow entropy production will manifest itself as a chemical (segregation) phenomenon.

D. Consequences of Diffusion Inhibition

Having proposed that the magnetic field inhibits diffusion, the effect of this phenomenon on the concentration gradient ahead of an advancing solid - liquid interface must be considered. The concentration gradient ahead of an advancing interface is shown schematically in Figure 21. If the magnetic field inhibits diffusion of the solute atoms, the mass transfer will tend from one of diffusion to one of forced convective - viscous flow. Thus, a "pile - up" of solute atoms at the interface will result and the solute concentration will change from the normal form, C_N, to C_F shown in Figure 21. If the equilibrium solidification temperature is plotted for this "field" concentration curve using the unchanged phase diagram, a curve similar to that illustrated by T_μ is obtained. An equilibrium solidification temperature gradient such as T_μ is, however, incompatible with the heat flow requirements necessitated by the temperature boundary conditions.

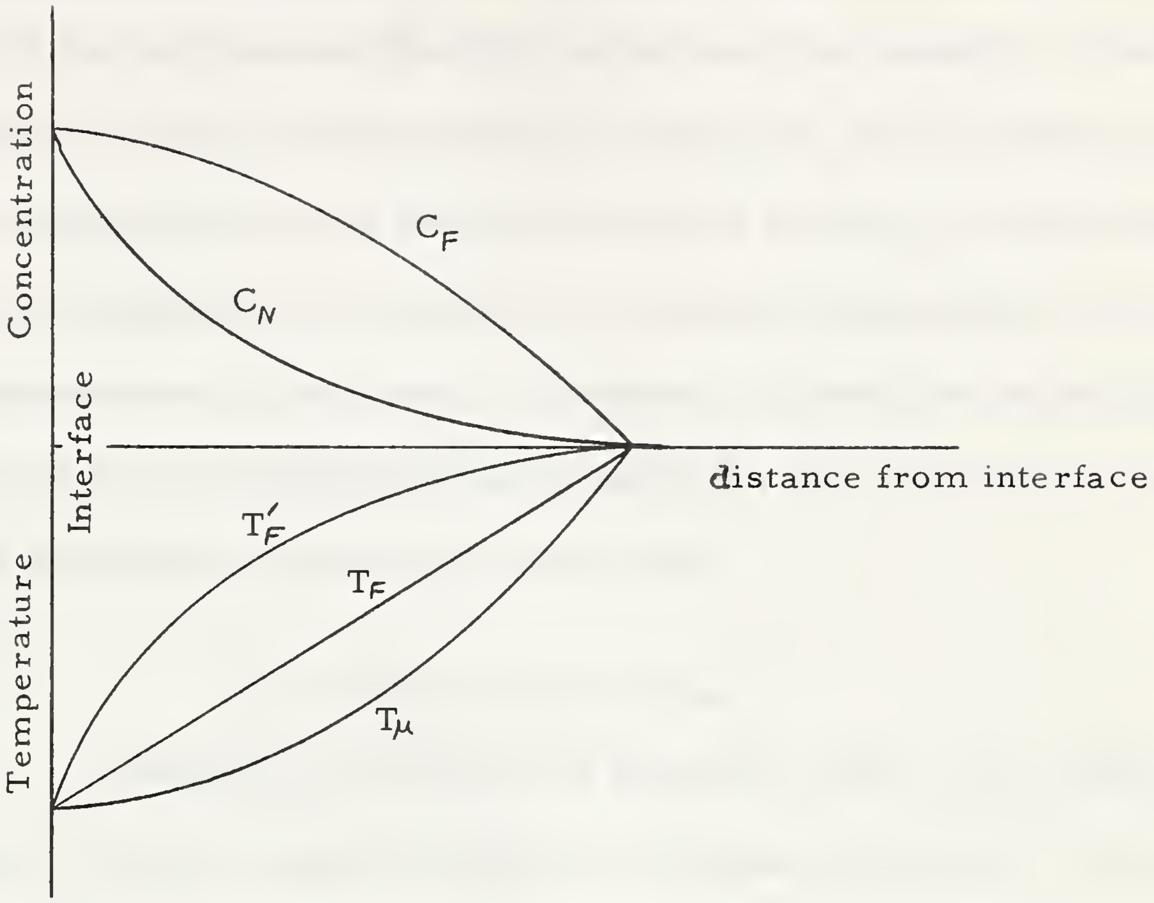

C_N - Normal concentration gradient in the liquid

C_F - Proposed concentration gradient in the liquid

T_μ - Solidification temperature for C_F using the unchanged constitutional diagram

T_F and T_F' - Solidification temperatures for C_F obtained by raising liquidus line of the constitutional diagram

Figure 21. Concentration Gradients and Temperature Distributions at the Solid - Liquid Interface

The temperature distribution at the sink must have the form $\partial^2 T/\partial x^2 < 0$, as this is the only solution possible for the heat flow equation. If the liquidus line takes the form of the dashed line in Figure 20, the constitutional requirements coupling the thermal and diffusion fields result in a temperature gradient of the form T_F or ever T_F', ie. one that is compatible with the heat flow requirements of the system. Therefore, in order for solidification to occur under the imposed diffusion constraint, the constitutional diagram must be altered as proposed (see Figure 20).

E. Energy Considerations

It remains to reconcile the proposed change in the constitutional diagram, which we suggest is effected via diffusion inhibition, with the local equilibrium principle. For equilibrium considerations the total or cohesive energy of the system must be examined. The cohesive energy of a lattice can be represented through the Schrodinger wave equation, using approximation methods for its solution. The cellular approximation of Wigner and Seitz has been applied with some success to bi- and multi-valent metals. The cohesive energy of a lattice, E_I, referred to its sublimated state is given by(38)

$$-E_I = E_0 + \frac{3}{5}\frac{h^2}{8m}\left(\frac{9}{4\pi^2}\right)^{2/3}\frac{Z^{2/3}}{r_0^2} + \frac{be^2}{r_0} \quad , \tag{15}$$

where E_0 is the zero point energy of the electron, Z is the valence of the metal, and r_0 is the radius of the unit cell in the sphere approximation. The second term is the average Fermi energy of the electrons and be^2/r_0 accounts

for the electron interaction energy per electron pair in any one atomic cell. Since r_o is proportional to $V_o^{1/3}$, the atomic cell volume, Equation (15) emphasises the relationship between the cohesive energy and the specific volume of a metal.

In a binary alloy system it is usually assumed that the free electrons exist in two sets of Fermi energy levels associated with the potential fields of the constituent ions.(39) The two sets of energy levels are superposed to give a single energy band of non - uniform density (providing the energy levels are different). There is a redistribution of electrons between bands to lower the total energy by an amount approximately equal to the bond energy of the system. This phenomenon of Fermi energy equilibration also occurs when two different systems are brought into mutual contact.(40) Varley(41) has shown that the radius of an atomic cell in alloys is approximately given by

$$r = r_o\left(1 + \frac{n}{Z}\right)^{2/9} , \qquad (16)$$

where n ($n \gtrless 0$) is the charge transfer. Therefore, redistribution of charge will result in an atomic volume change which will in turn affect the total energy of the system.

The proposed change in the constitutional diagram per se represents a departure from local equilibrium, and therefore an increase in energy. It is suggested that this energy increase is counterbalanced by a change in the specific volume of the liquid alloy which is due to transfer

of electrons across the solid - liquid interface in accordance with the principle that the Fermi levels of the two contiguous phases in equilibrium must be coincident. The specific volume change would be almost entirely in the liquid since the modulus of elasticity of the liquid is about 1/3 that of the solid. Any volume change in the solid would increase the overall strain energy of the system. Thus, local equilibrium can be restored at the interface through the process of electron transfer and specific volume increase or decrease in the liquid. This volume change proposal has been experimentally supported by Cahoon.(2) He found that it was possible to account for an increase in inverse segregation of Al - Cu alloys in a magnetic field only by altering the constitutional - specific volume relationship of the system.

VII. SUMMARY AND CONCLUSIONS

The present investigation of the effect of a magnetic field on solidification mechanisms, principally that of normal segregation and the transport processes involved therein, leads to the following conclusions:

(1) Solidification in a magnetic field increases the normal segregation in aluminum - 3 pct. copper alloys for certain freezing rates. The amount of segregation for rates from 3/4 to 2 inches per hour is increased by 12 pct. (the effective distribution coefficient is reduced from 0.76 to 0.67) and below rates of 1/2 an inch per hour the field has no observable effect. The effective distribution coefficients extrapolate to the equilibrium value at zero growth rate.

(2) A theory which considers the plasma - like properties of liquid metals, and which is based on the effect of a magnetic field on irreversible transport processes is developed to explain the results.

(3) The theory shows that diffusion inhibition caused by the magnetic field has the effect of raising the liquidus curve of the alloy system. This is shown to be compatible with heat flow requirements for the solidifying system in the presence of the thermal and diffusion constraint. Local equilibrium is restored at the interface through the process of electron transfer across the interface and the accompanying specific volume increase or decrease (in this case an increase) in the liquid alloy.

(4) Normal segregation results do not give quantitatively the extent of the

liquidus shift because the experimentally determined effective distribution coefficients are not directly related to the equilibrium distribution coefficient. The effect of the magnetic field inhibiting convective flow and diffusion will tend to increase K. However, a decrease of 12 pct. was observed in the effective distribution coefficient for solidification in the field. This indicates that the magnitude of the change in the equilibrium distribution coefficient is greater than the decrease of the effective distribution coefficient. Thus, it may be concluded that K_0 for Al - 3 pct. Cu alloys is decreased somewhat more than 12 pct. by a magnetic field of 34,000 oersteds.

BIBLIOGRAPHY

(1) D.R. Colton, Master's Thesis, University of Alberta, (1960)

(2) J.R. Cahoon, Master's Thesis, University of Alberta, (1963)

(3) J.S. Kirkaldy and W.V. Youdelis, AIME Trans., 212, 833 (1958)

(4) W.A. Tiller, K.A. Jackson, J.W. Rutter, and B. Chalmers, Acta Met., 1, 428 (1953)

(5) W.G. Pfann, AIME Trans.,

(6) J.A. Burton, R.C. Prim, and W.P. Slichter, J.Chem.Phys., 21, 1987 (1953)

(7) F.V.Dean, J.R. Kerr, and A. Hellawell, J.Inst.Metals, 90, 234 (1961 - 62)

(8) J.A. Burton, E.D. Kolb, W.P. Slichter, and J.D. Struthers, J.Chem.Phys., 21, 1991 (1953)

(9) D.Walton, W.A. Tiller, J.W. Rutter, and W.C. Winegard, AIME Trans., 200, 1023 (1955)

(10) W.A. Tiller and J.W. Rutter, Can.J.Phys., 34, 96 (1956)

(11) C.Wagner, AIME Trans., 200, 154 (1954)

(12) A.S.Yue and J.B. Clark, AIME Trans., 218, 55 (1960)

(13) F. Weinberg, AIME Trans., 227, 231 (1962)

(14) P. Niessen, W.A.M. Hewer and W.C. Winegard, Can.Met.Quart., 2, 341 (1963)

(15) O. Snellman and F.J. Burge, J.Sci,Inst., 26, 331 (1949)

(16) W.D. Lawson and S. Nielsen, Preparation of Single Crystals, Butterworths Scientific Publications, London (1958) p. 14

(17) W.W. Scott, Standard Methods of Chemical Analysis, Vol. 1, D. Van Nostrand Company Inc., (1939) p. 40, 368

(18) A.S. Gupta, Appl.Sci.Res., 9A, 313 (1960)

(19) C. Kittel, Introduction to Solid State Physics, John Wiley & Sons, Inc., New York, (1957) p. 580

(20) Handbook of Chemistry and Physics, 44th Edition, (1962 - 63) p. 2731

(21) A. Wolfe and A. Goetz, Phys.Rev., 46, 1095 (1934)

(22) H. Jones, Proc.Roy.Soc., A144, 225, (1934)

(23) G. Dresselhaus, Phys.Rev., 114, 736 (1959)

(24) J.E. Drummond, Plasma Physics, McGraw - Hill Book Company Inc., (1961) p. 1

(25) T.G. Cowling, Magnetohydrodynamics, Interscience Pub. Inc., New York, (1957) p. 3

(26) L. Spitzer, Physics of Fully Ionized Gases, Interscience Pub. Inc., New York, (1956) p. 94

(27) Ibid., p. 24

(28) Ibid., p. 38

(29) Ibid., p. 40

(30) T.G. Cowling, Magnetohydrodynamics, Interscience Pub. Inc., New York, (1957), p. 103

(31) H. Eyring, J.Chem.Phys., 4, 283 (1936)

(32) S.R. de Groot, Thermodynamics of Irreversible Processes, North Holland Publishing Co., Amsterdam, (1951) p. 196

(33) W.B. Brown, Trans.Faraday Soc., 54, 772 (1958)

(34) J.S. Kirkaldy, Can.J.Phys., 38, 1343 (1960)

(35) J.S. Kirkaldy, Can.J.Phys., 38, 1356 (1960)

(36) S.R. de Groot, Plasma Physics - Accelerators - Thermonuclear Res., 2, 188 (1961)

(37) C. Kittel, Introduction to Solid State Physics, John Wiley & Sons, Inc., New York, (1957) p. 149

(38) A.H. Wilson, The Theory of Metals, Cambridge Univ. Press, (1954) p. 74

(39) H. Friedman and W.W. Beeman, Phys.Rev., 58, 400 (1940)

(40) A.J. Dekker, Solid State Physics, Prentice - Hall Inc., (1957) p. 230

(41) J.H.O. Varley, Phil.Mag., 45, 887 (1954)

B29815